Sustainable aviation fuel (SAF) production through power-to-liquid (PtL): A combined techno-economic and life cycle assessment

Maria Fernanda Rojas-Michaga [a,*], Stavros Michailos [b], Evelyn Cardozo [c], Muhammad Akram [a], Kevin J. Hughes [a], Derek Ingham [a], Mohamed Pourkashanian [a]

[a] Energy 2050, Department of Mechanical Engineering, Faculty of Engineering, University of Sheffield, Sheffield S3 7RD, United Kingdom
[b] School of Engineering, University of Hull, Hull HU6 7RX, United Kingdom
[c] Centro Universitario de Investigaciones en Energías, Faculty of Science and Technology, University Mayor of San Simon, Cochabamba, Bolivia

ARTICLE INFO

ABSTRACT

The current research critically evaluates the technical, economic, and environmental performance of a Power-to-Liquid (PtL) system for the production of sustainable aviation fuel (SAF). This SAF production system comprises a direct air capture (DAC) unit, an off-shore wind farm, an alkaline electrolyser and a refinery plant (reverse water gas shift coupled with a Fischer-Tropsch reactor). The calculated carbon conversion efficiency, hydrogen conversion efficiency, and Power-to-liquids efficiency are 88 %, 39.16 % and 25.6 %, respectively. The heat integration between the refinery and the DAC unit enhances the system's energy performance, while water integration between the DAC and refinery units and the electrolyser reduces the demand for fresh water. The economic assessment estimates a minimum jet fuel selling price (MJSP) of 5.16 £/kg. The process is OPEX intensive due to the electricity requirements, while the CAPEX is dominated by the DAC unit. A Well-to-Wake (WtWa) life cycle assessment (LCA) shows that the global warming potential (GWP) equals 21.43 gCO_{2eq}/MJ_{SAF}, and is highly dependent on the upstream emissions of the off-shore wind electricity. Within a 95 % confidence interval, a stochastic Monte Carlo LCA reveals that the GWP of the SAF falls below the UK aviation mandate treshold of 50 % emissions reduction compared to fossil jet fuel. Moreover, the resulting WtWa water footprint is 0.480 l/MJ_{SAF}, with the refinery's cooling water requirements and the electricity's water footprint to pose as the main contributors. The study concludes with estimating the required monetary value of SAF certificates for different scenarios under the UK SAF mandate guidelines.

1. Introduction

Growing concerns over global warming have led to increased awareness among different sectors, including the aviation industry. The Air Transport Action Group (ATAG) has set an ambitious target for 2050 of reducing the net annual emissions to half of what they were in 2005.

Achieving this target requires various action plans, including the use of sustainable aviation fuels (SAF) [1]. Bio-based fuels have been proposed as a short to medium-term alternative to fossil jet fuel. Environmental assessments have shown that for different feedstock and bio jet-fuel production technologies, the resulting greenhouse gas (GHG) emissions are significantly lower compared to fossil-derived fuels. To support and increase the share of SAF utilization in the total kerosene consumption, some countries such as Germany and the United Kingdom are formulating and implementing supporting policies. However, producing SAF on a large scale requires strategies to meet the proposed production targets. The main challenge associated with this is the availability of large quantities of high-quality feedstock, as land-use changes may have greater environmental consequences than petroleum-based fuels. Therefore, the feedstock selection for SAF production is limited to waste biomass [2]. While some countries have large amounts of residual biomass, others are unable to meet their own needs and must import it from other regions. Given that LCAs have shown that biomass-derived fuels are transport-intensive [3], focusing on the availability is not a sustainable strategy. As a result, having a diverse SAF supply chain is critical in order to meet the aviation market's sustainability criteria.

PtL production has been proposed in this context as a promising and scalable alternative SAF production pathway. This process combines CO_2, water, and renewable energy to produce SAF with properties that are similar to those of fossil jet fuel. The three major steps that comprise this pathway are the CO_2 capture, hydrogen production (generally from water electrolysis), and hydrocarbons synthesis and conditioning process [4]. Hydrocarbons synthesis can be performed through two different pathways: Fischer-Tropsch (FT) synthesis, or methanol to jet fuel; however, the FT process outperforms the methanol pathway since the use of blends containing 50 % of FT-derived SAF and 50 % of conventional jet fuel is ASTM-certified as drop-in. In terms of CO_2 sources, direct air capture (DAC) is gaining popularity due to its potential for mitigating anthropogenic GHG emissions from dispersed sources while ensuring flexibility in plant location selection [5]. Furthermore, when coupled to low carbon footprint energy, the use of DAC for fuel synthesis may be able to close the carbon cycle and lower CO_2 emissions [6]. More studies that evaluate a suitable integrated Power-to-jet fuel system from a techno-economic and environmental standpoint are thus required to justify this carbon footprint reduction and other economic and environmental claims while providing quantified feasibility data for policymakers or other aviation-related organisations.

The PtL concept for the production of FT-derived fuels is a relatively new alternative pathway. As for now, only a few demonstration plants have been constructed [7,8], and more studies are required to fully understand the performance of the scenario for a larger commercial scale plant. Some studies have focused on the technical aspect of the scenario through process modelling [9–12], while others further proceeded to economic assessments [12–15] to find the levelised cost at which these fuels could be feasible. Similarly, there are other studies focusing on the environmental performance of this production pathway, from which most of them focused on the estimation of the global warming potential (GWP) [15–18].

There has been only a little research that specifically analyses the production of SAF from a PtL process that is available. Economic assessments are typically conducted to evaluate the cost and economic feasibility of such a process, taking into account the cost of the feedstock, energy, and capital investments needed. Three different reports produced by Batteiger et al. [19], Schmidt et al. [20], and Fasihi et al. [21] assessed the economic and environmental performance of PtL-derived SAF. By analysing short- and long-term scenarios, these reports determined whether this method was economically viable. Similar to this, their environmental assessments focused on the emissions of greenhouse gases and other pollutants associated with the life cycle of the PtL-SAF. Generally, these assessments conclude that PtL is a more sustainable option than other SAF production technologies, with significantly lower GWP, and a much higher minimum jet fuel selling

price when compared to the gate price of conventional jet fuel. Additionally, a comprehensive LCA was performed by Micheli et al. [22], who studied the environmental assessment of various PtL SAF process configurations and calculated the GWP, alongside other environmental factors, such as the water footprint and land use. The foreground data used in the LCA of this study, which is solely an environmental assessment, derives from previous available studies related to the production of PtL fuels.

The research mentioned above is valuable for understanding the economic and environmental performance of PtL-SAF, but they lack a comprehensive process modelling and integration. Without such models, it is difficult to analyse the effect of various parameters, including system design, operation, and energy generation, on the mass and energy performance, as well as the economic and environmental indicators. In particular, these models could improve our understanding of low TRL units, such as the Reverse Water Gas Shift (RWGS) reactor. Moreover, there are few studies that examine SAF production from an integrated techno-economic and environmental perspective, and early studies did not consider the possibility of process integration. By developing detailed models of different sections of the system, it may be possible to achieve synergistic integration that improves technical, economic, and environmental performances [23]. In this regard, given the growing interest in PtL processes, and as for the aforementioned knowledge gaps, to the best of our knowledge, this is the first study of its kind that jointly analyses the technical, economic and environmental performance of the PtL for SAF production, based on comprehensive process models for an integrated DAC-electrolyser-process plant, based in the UK. Furthermore, most studies in the literature concentrate on FT configurations that generate diesel, naphtha, or simply syncrude. Further, the current study focuses on maximising the jet fuel yield that requires the use of additional units, such as hydrocracking and isomerization, as well as higher syngas recycling ratios [3].

2. Methodology

2.1. Capacity of the plant and potential plant location

The growing interest in producing SAF via the PtL route is reflected in the growing number of studies and projects being developed [24]. For example, a roadmap to support the development of the PtL-derived SAF has been proposed by the German government and industrial leaders targeting an annual production of 200,000 tonnes of SAF for regional utilization by 2030 [25,26]. In the same context, a public consultation has been released in the UK in order to lay the groundwork for a future SAF mandate [27,28]. Various SAF uptake scenarios were proposed to replace the UK aviation fuel demand in the short and long term (starting in 2025 until 2050). The UK government has set a target of replacing 10 % of fossil jet fuel by 2030. Given the PtL's low GHG emissions and future cost reductions, the government has stated its intention to promote PtL's technological and commercial development. Since the UK consumption of jet fuel estimated by 2030 equals 12.7 Mtonnes [29], and considering that the efuel's production potential has been estimated as 2.7 % of the 2030 jet fuel demand, an estimated 0.34 Mtonnes/year of PtL-derived SAF could be produced. Considering a coverage of 6 % of this SAF target, the production capacity of the plant of the present study is set as 2,500 kg/h of jet fuel [27].

The electricity requirements of PtL systems are significant [4,30], and this can have a major impact on the GWP of the resulting fuel. Therefore, in this study, the energy for the process is assumed to be supplied by a dedicated offshore wind farm. By 2019, capacities of onshore and off-shore wind farms in the UK, were 10 GW and 8.5 GW, respectively [31]; furthermore, there is a plan to increase off-shore wind capacity to 40 GW by 2030 [32]. Among the current UK operational offshore wind farms, the Teesside facility operated by EDF is responsible for producing 62 MW of electricity. BP has also announced plans to build a 60 MW facility for electrolysis-based hydrogen production in the same

region by 2025, with plans to increase the size to 500 MW by 2030 [33]. Due to the region's high wind potential, the integrated wind farm-electrolyser-DAC-process system of this study has been located in the Teeside region.

2.2. System description and modelling

The system is divided into three major sections, as depicted in Fig. 1: the DAC unit, water electrolysis, and the refinery plant (syngas and fuel synthesis, as well as conditioning). The process configuration has been set up to favour the production of middle distillates, especially jet fuel range hydrocarbons. The various sections are represented by models at operating conditions that have been determined as optimal [11,12,34,35]. More details on the sections of the system are given in the following sections.

2.2.1. Direct air capture

Various DAC technologies have been developed, with alkali hydroxide solutions in liquid scrubbing and VTSA (vacuum temperature swing adsorption) on supported sorbents achieving the most advancement [36,37]. The VTSA technology, also referred to as the low temperature DAC, was chosen for this study because of its modularity that facilitates scaling-up efforts. Another advantage is its ease of operation, as all steps of CO_2 capture occur in the same unit, and bed regeneration occurs at low temperature, allowing low-quality heat generated at different stages of the proposed process to be integrated with the DAC unit [37–39]. The sorbent used in low-temperature DAC technology is critical, but the lack of experimental and mathematical models that accurately describe their operation increases the uncertainty of their mass and energy performance [36]. In this study, an amine-functionalized adsorbent, i.e. APDES-NFC, is considered because it has been indicated to be similar to the sorbent used by Climeworks DAC technology [36].

The Toth model is used to represent CO_2 adsorption. The APDES-NFC sorbent is thought to behave by the physisorption mechanism, with chemisorption being ignored [36]. The temperature and partial pressure of CO_2 are the main driving forces in this model: the higher the temperature, the less CO_2 is adsorbed in the bed [40]. Moreover, it has been observed that relative humidity improves CO_2 adsorption; however, few experimental or modelling papers have attempted to investigate its effect on CO_2 adsorption [36,41]. The methodology proposed by Sabatino et al. [36] is used for this study because it is based on the empirical calculation of the dependence of temperature on relative humidity. Water co-adsorption, on the other hand, is unaffected by factors other than temperature and water content. The temperature-dependent "GAB model" is used to represent water adsorption [36]. The use of the

aforementioned models, as well as some ideal gas equations, allows the estimation of the amount of CO_2 and H_2O that are captured after a DAC bed operating cycle. Finally, a carbon capture fraction of 90 % (an average value determined at the Hellisheiði and Hinwil Climeworks plants) is assumed [6]. More information on these models can be found in Section S.1.1 of the Supplementary Materials. Finally, the energy consumption encompasses both, heat and electricity requirements. Particularly, energy demands for the APDES-NFC sorbent are assumed to be equal to the data provided by Deutz et al. [6], and therefore, the process created by Climeworks needs between 1.8 and 2.6 MJ_{el}/kg (electricity requirement) and between 5.4 and 11.9 MJ_{th}/kg (heat requirement) in which the lowest value indicates the future target, and the highest the current consumption.

2.2.2. Off-shore wind farm and electricity supply

A dedicated offshore wind farm will be providing electricity to the integrated system. The wind speed profile is not constant and consequently the power generation fluctuates. Hence, to estimate the power generation curve, the hourly wind profile of the selected location, Teeside, is obtained from the NASA/MERRA-2 website [42]. The chosen data is for the year 2021, and the geographic coordinates correspond to the Teeside wind farm operated by EDF. The software SAM is used for the estimation of the hourly energy generation, which is calculated from the adjusted wind speed profile, as well as with the selection of the nominal power generation (by defining the number of wind turbines). The selected wind turbine model is the Senvion 6.2 M126 offshore, due to its suitable operation between the speed ranges registered in the chosen location. The wind speed profile (see Fig. 2) is provided at 10 m
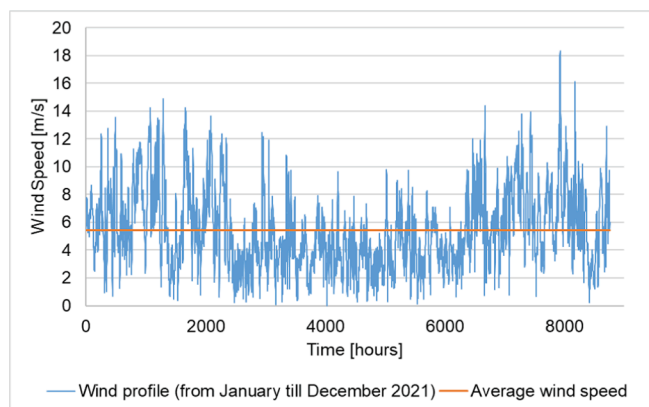

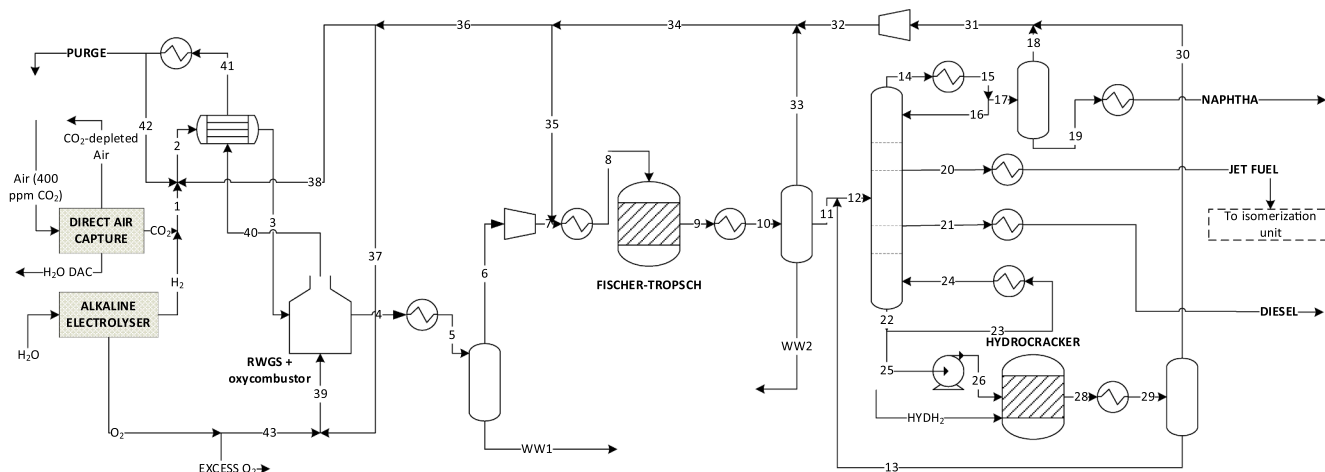**Fig. 2.** The wind speed profile for Teeside.

Fig. 1. Process flow diagram of the investigated PtL process for SAF production.

above the ground and therefore is adjusted with Equations (1) and (2) to a height of 80 m. Equation (1) estimates α, which is the power law exponent, and is calculated by using the mean wind speed (U_{ref}) and the height at which wind speeds have been collected. Equation (2) is the power law profile and finds the new speed values $U(z)$, at a specific height z.

$$\alpha = \frac{0.37 - 0.088\ln(U_{ref})}{1 - 0.088 ln\left(\frac{z_{ref}}{10}\right)} \tag{1}$$

$$\frac{U(z)}{U(z_{ref})} = \left(\frac{z}{z_{ref}}\right)^{\alpha} \tag{2}$$

For an enhanced operating performance, it is important that the electrolyser receives uninterrupted nominal power, which will also maximise its service life [43]. Annexing a battery bank to the wind farm could allow the storage of the excess power, and the supply of energy, when the power generated is lower than the required nominal. Although, few studies have assessed the techno-economic potential of this integrated wind farm-battery bank-electrolyser system for H$_2$ production [44–47]. Moreover, the design of such a system is time consuming since it is a multi-objective optimisation problem, with multiple solutions that have trade-offs between several technical, economic and environmental performance indicators, and due to this reason, this design is out of the scope of this study. Additionally, such hybrid wind farm-battery systems have shown lower energy efficiency and higher capital costs [44,45]. Therefore, to tackle the energy production fluctuation, the use of the grid network as a "virtual" storage system is proposed: when excess electricity is produced, electricity is injected into the grid, while in the case of lower power generation, the system takes electricity from the grid [44,48]. The wind farm is sized so that the average annual electricity generation equals the overall electricity demand of the whole PtL system. Further, the grid annual electricity consumption (and its inherent emissions) is offset by the injection of the wind farm excess electricity [48].

2.2.3. Electrolyser

Three main water electrolysis technologies can be mentioned: alkaline electrolyser (AE), proton exchange membrane (PEM) and solid oxide electrolysis cell (SOEC). Despite its lower performance, the AE was chosen for this evaluation due to its high TRL and potential for industrial scalability. Equation (3) depicts the electrolysis reaction and indicates a requirement of 9 kg of deionised water for the production of 1 kg of H$_2$. On considering, losses at several sections of the AE operation plant, such as water treatment (ion exchange), condensate, and others, the amount of water required to produce 1 kg of H$_2$ increases to 9.26 [49]. The ion exchange method of water treatment involves the adsorption of water contaminants into the ion exchange media (resin), which is disposed of or regenerated on a regular basis [50].

$$H_2O \rightarrow H_{2(g)} + \frac{1}{2}O_{2(g)} \tag{3}$$

Larger electrolysis capabilities might be accomplished by connecting multiple AE stacks, while also modifying the balance of the plant's elements to the desired size, as commercially available AE stacks have a maximum capacity of 2.5 MW [49]. The electrolyser's efficiency is constrained because some of the electricity it receives is converted to heat. This heat must be continuously evacuated in order to maintain the electrolyser's isothermal operation. Typically, cooling water is utilised for this, and for the sake of increasing the energy efficiency, we assumed that it is also used for district heating at low temperatures. Another additional element of the balance of the plant of the AE electrolyser includes the AC-DC converter, where around 6 % of the energy is lost [49]. All the operational parameters and energy and mass balances considered for this study are taken from a 100 MW electrolyser as presented in the work of Holst et al. [49], and adjusted to the required electrolyser capacity. With regards to the operating pressure, it has been
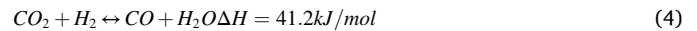
found to have low influence in the efficiency of the stack, and it could be set according to the downstream application requirements [51,52]. Even so, the pressurised AE is described as a system with several operating issues with a larger cost due to the need of resistant to high pressure materials; therefore, it is regarded as rather undesirable, and an atmospheric system with downstream compression is preferred [49].

2.2.4. Process plant

The refinery process model has been developed in Aspen Plus with the aim of estimating the mass and energy balances of the proposed process configuration. Due to its suitability for gas processing, refinery, and petrochemical plants, the Peng-Robinson-Boston-Mathias was chosen as the thermodynamic property package [53]. In the following sections, the main functional units are explained.
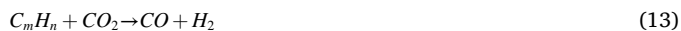
a) Reverse Water Gas Shift

In the refinery, the reverse water gas shift reactor is a crucial component since it primarily enables the catalytic conversion of the CO$_2$/H$_2$ mixture into syngas. Generally, RWGS reactors operate at a temperature ranging from 700 °C to 1000 °C, and H$_2$ to CO$_2$ ratios of 1:1 to 3:1 [54]. Chemically, the RWGS process is represented by a main reaction (Equation (4) that is thermodynamically favoured at high temperatures. In addition, side reactions (Equation (5), Equation (6), Equation (7) and Equation (8) occur and are responsible for the production of methane and soot deposition. In order to eliminate the energy penalty of the pre-FT compression unit, it is generally recommended that the RWGS reactor be operated at the same high operating pressure as the downstream FT reactor [55]. However, it has been observed that high pressure increases the rate of the methanation reaction [13,55], which has a negative impact on the energy efficiency of the process and outweighs the advantages of a high pressure RWGS reactor. The studies by Adelung et al. [10,13] used process modelling method to analyse this effect. The ideal operating pressure and temperature ranges that increase de PtL efficiency and the CO$_2$/H$_2$ conversion efficiencies have been determined by the authors through a parametric analysis.

$$CO_2 + H_2 \leftrightarrow CO + H_2O \Delta H = 41.2 kJ/mol \tag{4}$$

$$CO_2 + 3H_2 \leftrightarrow CH_4 + H_2O \Delta H < 0 \tag{5}$$

$$CO_2 + 4H_2 \leftrightarrow CH_4 + 2H_2O \Delta H < 0 \tag{6}$$

$$2CO \leftrightarrow C + CO_2 \Delta H > 0 \tag{7}$$

$$CH_4 \leftrightarrow C + 2H_2 \Delta H < 0 \tag{8}$$

The recycling of the unreacted syngas from the FT unit to the RWGS is another topic of uncertainty. Although recycling boosts the efficiency, the presence of light hydrocarbons raises the level of operational unpredictability. Various approaches to modelling the decomposition of these light hydrocarbons have been used in previous studies, with a majority assuming an equilibrium conversion inside the RWGS reactor (Equations (9)–(13)). However, there is a lack of kinetic models and experimental data to analyse the effect of the conversion of these components on the selectivity of the RWGS reaction, or whether they can cause any operating problem. The only experimental work analysing the effect of the recycling of hydrocarbons over the performance of the RWGS is the one performed by Wolf et al. [56]. They found that CH$_4$ was not responsible of any coking up to a CH$_4$/CO$_2$ ratio below one. However, replacing CH$_4$ by C$_3$H$_8$, is responsible of thermal and catalytic coking. Catalytic coking increases up to 700 °C and decreases above this temperature. Thermal coking, on the other hand, increases with higher temperatures but can be suppressed by the addition of water [56]. Another approach considers prior reforming of these hydrocarbons with an ATR unit, which may solve the uncertainty problem at the expense of higher CAPEX and lower process efficiencies [54].
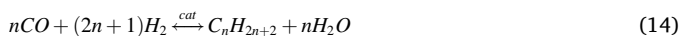
$$C_mH_n \rightarrow C_x + zH_2 \tag{9}$$

$$C_mH_n \rightarrow C_xH_y + zH_2 \tag{10}$$

$$C_mH_n + O_2 \rightarrow CO + H_2 \tag{11}$$

$$C_mH_n + H_2O \rightarrow CO + H_2 \tag{12}$$

$$C_mH_n + CO_2 \rightarrow CO + H_2 \tag{13}$$

Based on the information presented above, the operating conditions selected for this study are 850 °C and 5 bar [54] for the "minimization of Gibbs energy modelling" of the RWGS unit, assuming that the operating conditions and reactor geometry are adjusted to reach the equilibrium stage [10,11]. As a consequence, under these operating conditions, it is assumed that catalytic coking does not occur and due to the presence of moisture in the recycling gas, thermal coking is considered negligible. The same approach as Adelung et al. [13] has been taken in terms of the source of energy for the RWGS reactions. Thus, the RWGS reactor is designed as a steam-reforming reactor, which means that the catalyst is packed inside the tubes, which are then placed inside the furnace, where oxy-combustion provides heat to the system. The RWGS reactor must be made of a high-quality metal or alloy (reactions above 850 °C) that can withstand temperatures as high as 1200 °C [57]. It is also worth noting that following this reactor, the outlet streams are cooled and a biphasic separator is installed to remove water that could deactivate the FT catalyst [10].

b) Fischer-Tropsch

The FT reactor synthesizes hydrocarbons from syngas, obtaining a product that mimics the composition of crude oil. This chemical process occurs according to Equations (14) and (15), representing alkanes and alkenes synthesis respectively [58]. The operating conditions, the configuration of the FT reactor, as well as the catalyst have direct effect on the properties, composition and the hydrocarbons chain length [59]. To maximise kerosene production it is important to obtain long-chain hydrocarbons in the range of middle distillates, which could be attained by adjusting the operating conditions of the synthesis reactor at 240 °C and 25 bar, while using a cobalt-based catalyst [59].

$$nCO + (2n+1)H_2 \xleftrightarrow{cat} C_nH_{2n+2} + nH_2O \tag{14}$$

$$nCO + 2nH_2 \xleftrightarrow{cat} C_nH_{2n} + nH_2O \tag{15}$$

There are several approaches for the modelling of the FT reactor, for this study, the kinetic model derived by Marchese et al. [60] has been chosen. The proposed model is a carbide mechanism model which was validated by the authors using experimental data obtained from a tubular fixed-bed reactor filled with Co-Pt/γ-Al$_2$O$_3$ catalyst [60], with a length that determines a CO per pass conversion of 75 %. This model includes some modifications to account for the main deviations from the Anderson-Schulz-Flory (ASF) distribution including higher methane selectivity, lower ethylene selectivity, and inclusion of olefins production. Refer to Section S.1.2 of the Supplementary Materials for more information on the carbide model and its integration into the Aspen Plus model.

c) Syncrude upgrading section and unreacted syngas recycling

The FT reactor's output requires additional processing to yield commercial hydrocarbon fractions, such as naphtha (C$_5$ to C$_7$), kerosene (C$_8$ to C$_16$), and diesel (C$_17$ to C$_20$). To accomplish this, a series of cooling and separation stages are used, yielding three phases: 1) unreacted syngas + light hydrocarbons, 2) liquid hydrocarbons, and 3) condensed water. The liquid hydrocarbons are separated in an atmospheric distillation column, and the heavy fraction (C$_{21+}$) is further processed to increase the final yield of middle distillates. As a result, the waxes are sent to a hydrocracking reactor, which runs on hydrogen and configured to maximise the jet fuel output [61,62]. More details about the assumed operating conditions of this reactor can be found in previous work by the authors [63].

To increase efficiency and productivity, the refinery plant must be set up to recycle unreacted gases [9–12]. More than one recycling stream can be sent back at various stages of the process and for various purposes, as shown in Fig. 1:

- One stream is recycled just before the FT reactor to ensure that its inlet has an inert content of 25 % for thermal stability inside the reactor [9].
- The second stream generates heat for the endothermic RWGS reactions, by its oxy-combustion in the RWGS reactor, which is similar to a steam reformer unit [10]. The oxygen coming from the electrolyser is used in stoichiometric amount ($\lambda = 1$), and the resulting flue gas is cooled further for energy recovery before being partially recycled to the oxy-combustor, with the goal of lowering its temperature to 1200 °C. Finally, the other flue gas fraction is mixed with the fresh CO$_2$ and H$_2$, which is then directed to the RWGS reactor after further heating.
- Finally, the third unreacted gas stream fraction that remains after the split of the required streams mentioned above, is also mixed with the fresh CO$_2$ and H$_2$, before the RWGS reactor.

2.2.5. Heat integration

The process is heat-integrated to maximise plant energy efficiency while reducing the use of hot and cold utilities. To that end, the software Aspen Energy Analyzer (AEA) is used to perform a Pinch Point analysis. The process and property information of the process streams are sent to the AEA model, while the energy requirements for the DAC and electrolyser are manually entered. The DAC unit requires heat for its operation during the desorption stage. An increase of the bed temperature diminishes the working capacity of the solid sorbent, and therefore, CO$_2$ and H$_2$O are released. For the Climeworks DAC unit, the desorption occurs at low pressure and moderate temperature. Therefore, a low quality heat source, such as medium or low pressure steam, could be integrated with the DAC system. The latest information provided by Climeworks, shows that the heat requirement is equivalent to 11.9 MJ$_{thermal}$/kg of CO$_2$ captured [6]; however, Climeworks has also claimed that, due to the continuous improvement and development of the sorbent materials, this heat requirement could be reduced to 5.4 MJ$_{thermal}$/kg of CO$_2$ [6]. The electrolyser, in contrast, generates heat. The heat released is used for a heat district system in the same manner as in von Hepperger's study [64]. It is assumed that the electrolyser operates at 70 °C [49], and this can be used in a 4th generation or low-temperature district heating system, where the supplied and returned temperatures are 60 °C and 35 °C, respectively[65].

2.2.6. Water integration and cooling water system

When it comes to water integration, different parts of the system have the capacity to produce water that could be used to meet the needs of different sections of the system, such as the hydrogen production island. The electrolyser requires to be cooled with cooling water, as indicated in the section above, in order to run at an isothermal temperature of 70 °C. The cooling set-up, however, resembles a dry-cooling system because the heat generated by the electrolyser will be used for district heating. This indicates that the cooling water cycles in a closed loop, never needing make-up water and never creating waste water [50]. As a result, the total ratio of 9.26 kg of H$_2$O to 1 kg of H$_2$ remains constant. Furthermore, it is worth noting that the water requirements are primarily derived from the air (captured alongside CO$_2$ at the DAC unit), and from the RWGS and FT reactors, where it is synthesized as a by-product. In comparison to tap water, the total dissolved solids (TDS) level of air-derived water is roughly ten times lower [66,67], and as a result, less sewage sludge will be produced. On the contrary, given that the water produced in the PtL process will contain some hydrocarbons, extra treatments may be necessary before its integration.

Moreover, a generic assumption of the amount of water that is lost from the cooling water network of the process plant is not sufficient, and therefore, a more detailed estimation is necessary and it is calculated

according to the following equations:

$$Makeupwater = EvaporationLoss + DriftLoss + Blowdown \quad (16)$$

The evaporation loss is calculated using Equation (17) and is caused by water evaporation when cold dry air comes into contact with hot cooling water. Where evaporation is assumed to be 1 % of circulation flow for every 10 °F (5.56 °C) rise between the outlet and inlet across the tower. Wind and relative humidity, among other factors, must be corrected. A factor of 0.85 is a reasonable approximation. If the climate is particularly moist, the value may fall to 0.65; if the climate is extremely dry, the value may rise to 1.0–1.2 [68].

$$EvaporationLoss = \left(0.85 * \left(\frac{1}{100}\right) * \Delta T\right) * \left(\frac{1}{10}\right) * CirculationFlow \quad (17)$$

Drift loss is water entrained in the tower discharge vapours, and can range between 0.1 and 0.2 % of the circulation flow. For a conservative scenario, 0.2 % is assumed. Finally, in order to reduce the system solids concentration, blowdown discards a portion of the concentrated (due to evaporation) circulating water. The number of concentration cycles required to limit scale formation can be used to calculate the blowdown, as indicated in Equation (18) [68]. For a conservative scenario, we assumed four cycles [69].

$$BlowdownLoss = \frac{EvaporationLoss}{Cyclesofconcentration - 1} \quad (18)$$

2.3. Performance indicators

To quantify the performance of the proposed process configuration, the following mass and energy performance indicators are calculated:

- Carbon fixation, also known as carbon conversion efficiency (η_C), is represented by Equation (19) and accounts for the conversion of the carbon content in the feedstock by relating the moles of carbon ($\dot{n}_{C,products}$) of the products to the moles of carbon of the feedstock ($\dot{n}_{C,feedstock}$) [13,35,70].

$$\eta_C = \frac{\dot{n}_{C,hydrocarbons}}{\dot{n}_{C,feedstock}} \quad (19)$$

- Hydrogen efficiency, as calculated by Equation (20), indicates the conversion of hydrogen entering the system's boundaries into the desired fuel products. This is determined by the ratio of the hydrogen content of the hydrocarbon over the hydrogen content of the feedstock [13].

$$\eta_H = \frac{\dot{n}_{H,hydrocarbons}}{\dot{n}_{H,feedstock}} \quad (20)$$

- Power to liquid efficiency (η_{PtL}), represented by Equation (21), relates the energetic content of the produced fuel ($\dot{m}_{jetfuel} \bullet LHV_{fuel}$) to the total energy input of the system, which is composed by the electrolyser's power requirement (P_{El}) and the power used for the process (P_U) [10,71].

$$\eta_{PtL} = \frac{|\dot{m}_{fuels} \bullet LHV_{fuel}|}{P_{El} + P_{DAC} + P_{process}} \quad (21)$$

2.4. Economic evaluation

Important economic indicators, such as CAPEX, OPEX and MJSP, will be calculated in order to obtain numerical results that could be comparable with other SAF production scenarios. The MJSP is defined as the SAF price at which the NPV is zero [72,73]. For this estimation, a discounted cash flow analysis (DCFA) is used; Table 1 contains the main financial parameters and assumptions. At the same time, the *nth* plant

Table 1
Parameters for conducting the discounted cash flow analysis [75,76].

Location	United Kingdom
Plant life	20 years
Currency	£
Base year	2020
Plant capacity	2,500 kg SAF/h
Discount rate	10 %
Federal tax rate	30 %
Construction period	3 years
First 12 months' expenditures	10 % of FCI
Next 12 months' expenditure	50 % of FCI
Last 12 months' expenditures	40 % of FCI
Depreciation method	Straight line
Depreciation period	10 years
Working capital	5 % of FCI
Start-up time	6 months

*FCI = Fixed Capital Investment.

assumption is adopted in order to avoid unnecessary artificial inflation of project costs inherent to the uncertain characteristics of pioneer plants [73,74].

2.4.1. CAPEX estimation

Equation (22) [73,77] is used to adjust the Purchase Equipment Cost (PEC) for units at different capacity. *C* denotes the cost of the unit at the actual capacity *S*, while C_0 is the base cost at a specific base size S_0 or capacity. The scaling capacity factor *f* has different values depending on the type of process equipment, and its goal is to reflect the effect of economies of scale [73].

$$C = C_0 \left(\frac{S}{S_0}\right)^f \quad (22)$$

Equation (23) is used to adjust the calculated PEC at different economic base year. $C_{baseyear}$ and $index_{baseyear}$ correspond to the base year of the study while the other variables, C_0 and $index_0$, refer to the year in which the original cost was obtained. The indices are taken from the "Chemical Engineering Plant Cost Index (CEPCI)" that serves as an important tool for chemical-process-industry projects in the adjustment of equipment price from one year to another. When the original prices of the equipment were not reported in GBP (£), a conversion factor was applied, corresponding to the year where this equipment price was detailed. Table S.3 of the Supplementary Materials contains information about the equipment cost estimation parameters.

$$C_{baseyear} = C_0 \left(\frac{index_{baseyear}}{index_0}\right) \quad (23)$$

Different cost estimations for low TRL technologies, such as DAC, come with more uncertainty and direct, indirect costs, as well as operating and maintenance costs, should not be estimated by using the factors applied in cost estimation of nth plant technologies. Regarding the AE, Researchers at Germany's Fraunhofer ISE have estimated the costs for both AE and PEM electrolysers, finding that the former has bigger margins for cost reduction. According to this report, the costs of a large scale AE with a capacity of 100 MW could drop from €663/kW in 2020 to €444 in 2030 [49]. Herein, we have used the 2020 value for the cost estimation of the AE.

- **Direct air capture cost:** There is a great deal of uncertainty surrounding the present and future costs of DAC units. Among the various assessments developed for DAC cost estimation, the National Academies of Science [78] and Young et al. [79] are the only assessments that thoroughly describe the breakdown of the capital and operating expenditures for relatively high TRL DAC technologies; solid sorbents by Climeworks among them. In this sense, the methodology adopted by Young et al. [79] was considered for the present study. Young et al. [79] determined that long-term Gigatonne CO_2-

scale DAC plants would result in lower costs than first-of-a-kind. The approach taken into account by the authors considers a first-of-a-kind (FOAK) solid sorbent DAC unit, the CAPEX and OPEX of which were estimated for a 0.96 ktonneCO_2/y unit (identical capture rate with the Hinwil plant operated by Climeworks). Then, CAPEX, fixed operating and maintenance costs (fixed OPEX costs), and variable costs (variable OPEX costs) are scaled up to the required plant capacity by using learning rates. Since the main intention of this study is to estimate costs for CO_2 capture, transport and storage, the CO_2 capture was recalculated by using the approach proposed by the original source [79]. More details on the calculations could be found in Section S.3 of the Supplementary Materials.

- **Reverse Water Gas Shift reactor:** Due to the novelty of this technology it is challenging to find a reliable equipment price. The considered PEC was taken from the work of Adelung et al. [13]. They developed an approach that is sensible to the operating conditions of the RWGS system. Since the operating conditions of our system are closer to the ones used by these authors, the same cost of the RWGS reactor was considered; nevertheless, the capacity was adjusted to the required for this system, by assuming a generic scaling factor of 0.65 due to the lack of relevant data (Table S.3).

Based on the calculated PEC, as well as on the methodology depicted in Table S.4 of the Supplementary Materials, it is possible to estimate the Total Direct Costs (TDC) and Indirect Costs (IC) [80]. The Fixed Capital Investment (FCI) is then calculated as the sum of TDC and IC. The interest during construction is calculated using 10 %, 50 %, and 40 % investments at a 10 % interest rate. Then, the CAPEX is estimated by adding the start-up cost and the interest during construction, while the working capital is considered as 5 % of the CAPEX.

2.4.2. OPEX estimation

As shown in Table S.5 of the Supplementary Materials, the OPEX (operating expenses) or manufacturing costs are calculated by adding the estimated values of fixed operating and maintenance costs (FOM), variable operating costs (VC), and plant overhead costs. VC is calculated by adding the prices of raw materials, utilities, and catalysts, which are summarised in Table S.5.

The levelised cost of the offshore wind electricity is calculated by the SAM software, following the calculations of the power generation curve explained in Section 2.2.2. Because continuous supply of electricity via wind turbines is not possible, the grid is used as a "virtual storage" of electricity (Section 2.2.2). Policies regulating this dynamic wind farm-grid interaction were not clearly found for the UK. Assuming a similar scheme as in existing net-metering policies (generally applied for small/medium scale generators of renewable energy connected to the grid), the generation costs of the electricity going and coming from the grid are offset. Given the private nature of the companies that own and operate transmission and distribution networks, a fee for network costs, must be paid for electricity drawn from the grid [81]. According to Eurostat [82], this fee is equal to 0.009 £/kWh for a UK-non-household consumer with electricity consumption above 150,000 MWh in 2019. In UK, the network costs are generally passed to the consumers [83,84], and therefore no charges for injecting energy to the wind farm are considered.

In turn, the labour is calculated using the empirical relationship, Equation (24), proposed by Peters et al. [85]. Where "plant capacity" refers to the amount of jet fuel produced, expressed in kg/h, "$n_{processsteps}$" or the number of process steps, refer to the number of sections within the process, where significant chemical and/or physical changes occur. In addition, "$h_{plantoperation}$", refers to the annual operating hours of the plant, which is considered to be 8,000 h/year. Once the hours of labour "h_{labour}" are estimated, the cost of the labour is calculated by considering that the price of one hour of labour is equal to 15 £/h [85–87].

$$h_{labour} = 2.13 \times plantcapacity^{0.242} \times n_{processsteps} \times \frac{h_{plantoperation}}{24} \quad (24)$$

It is important to mention that the OPEX of the DAC unit is not calculated according to this conventional methodology. Instead, the approach followed by Young et al. [79] is adopted as explained for the DAC-CAPEX section. The methodology followed by these authors calculates the OPEX in two stages. The energy requirements are considered from the values stated from Climeworks in the study of Deutz et al. [6]. The DAC unit does not necessitate external heating since the amount of heat that is necessary for the process is provided by the steam produced at the FT reactor. On the other hand, the DAC electricity is considered in the economic calculations. For more details about this estimation, Section S.3 of the supplementary materials provides more information of the adopted approach. Additionally, for the estimation of the OPEX, it is important to mention that for the AE, it is necessary to change the stack every ten years, and therefore this cost is as well considered and calculated according to the following Equation (25) [88]

$$Alk_{repl.} [£/kW] = \frac{2}{3} * 0.4 * Alk_{CAPEX} \quad (25)$$

2.5. Life cycle assessment (LCA)

The Life Cycle Assessment (LCA) is performed according to the standardised approach outlined in ISO 14040 and 14044 to ensure the consistency and transparency of the LCA studies [89]. According to this approach, the LCA is comprised of four main steps: definition of the objective and scope of the study; construction of the inventory analysis; determination of the environmental impacts; and the interpretation of the results.

2.5.1. Goal and scope definition, functional unit

The goal of this LCA is to find the environmental performance of the integrated system, which represents a CO_2 utilisation scenario under the Power-to-aviation concept. The system boundaries are placed in a way that the LCA analyzes the whole supply chain until the combustion of the produced SAF, which is known as the Well-to-Wake (WtWa) analysis, as depicted in Fig. 3. Among the various environmental impacts, the global warming potential (GWP) is mainly assessed, which allows a comparison with existing SAF production pathways, as well as with regulating standards, such as the U.S. Renewable Fuels Standard (RFS) and the European Renewable Energy Directive II (RED II). These standards establish the required threshold for CO_{2eq} emissions reduction compared to those of conventional jet fuel, which is equal to 89 gCO_{2eq}/MJ and 94 gCO_{2eq}/MJ, for the RFS and the RED II, respectively [90,91]. Synthesized jet fuel can be considered as SAF when its inherent GWP achieves at least 50 % and 70 % GHG emissions savings when compared to fossil jet fuel, in compliance with the RFS [92] and the RED II [91], respectively. On the other hand, the UK government is planning that for SAF to receive credits under the SAF mandate, it will be required to achieve a 50 % GHG saving compared to a fossil fuel benchmark of 89 gCO_{2e}/MJ [28]. In addition, the water footprint is estimated, although there is currently no regulation towards this specific environmental impact.

The functional unit is selected on an energy basis, and therefore it is equal to 1 MJ of SAF while considering that the LHV of the SAF is equal to 42.8 MJ/kg [93]. This choice is made for ease of comparison of fuels with different origin when they have the same end use (e.g. combustion in the same aircraft) [94]. Additionally, SimaPro V.9.3.0.3 is used to conduct the LCA together with its built-in databases, such as Ecoinvent 3.6, which is a reliable source of background information.

2.5.2. Multi-functionality

Most systems face a methodological difficulty when it comes to the application of the LCA analysis on the production of multiple products, or by-products, since a decision needs to be made on how the
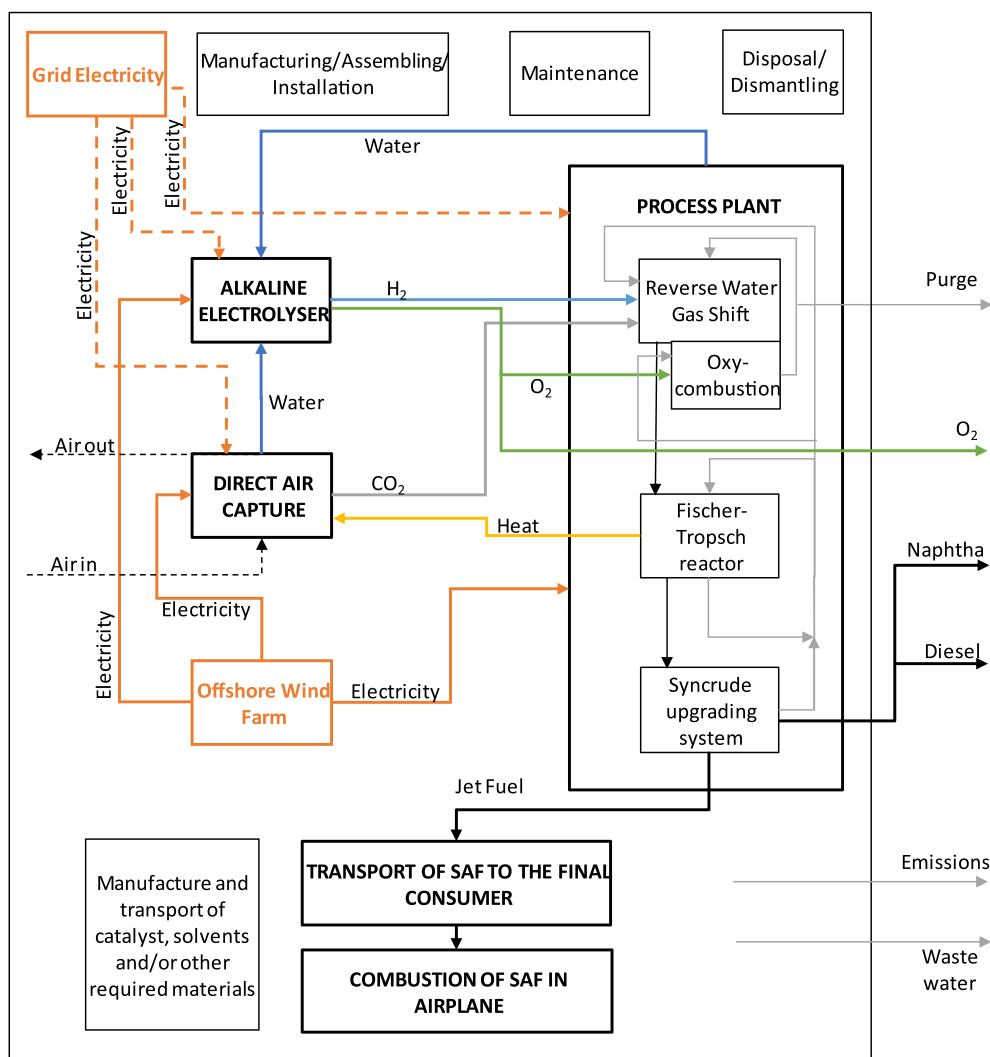
Fig. 3. The system boundaries for the LCA of the investigated SAF route.

environmental impacts will be distributed. As a result, the use of allocation methods is required, but their selection is challenging because they all produce results that differ significantly from one another [95]. An exhaustive list of allocation methods could result in a large number of options, given that some studies develop their own approaches. However, the most popular methodologies that could be mentioned include the allocation based on physical basis, such as mass, energy, exergy, among others; furthermore, economic allocation is also frequently applied, particularly when the economic value of the product is the driving force of the system. Finally, allocation by substitution, also known as system expansion, could be also found in some LCA, by crediting avoided emissions associated to the by-products that displaced similar but more environmental harmful products [96,97]. In this sense, the chosen methods for the multifunctional system of this study, will be the energy, as well as the exergy allocation, due to the energy content of the produced SAF and the by-products (naphtha, diesel) [95,98]. The base scenario is defined as the exergy allocation, which uses an exergy allocation at the refinery level, however, no allocation is applied in the electrolyser due to the reasons that are further explained in Section 2.5.3.2. The allocation approach based on system expansion is not further explored since this method is prone to calculate lower GHG emissions for substituted products with larger carbon intensities than the studied system [63,99].

2.5.3. Life cycle inventory (LCI) and description of the life cycle stages

The LCI for the described system is elaborated based on two primary data sources: The mass and energy balances produced through the process modelling in Aspen Plus, as well as from the literature-derived data. This information covers the normalised figures, as per the functional unit, for the DAC process, the electrolyser, as well as for the refinery plant. Moreover, the data includes information about the various waste streams and emissions produced throughout the indicated processes. The second data source is comprised of the required background data, which is mainly found in the Ecoinvent 3.6 database, as well as in the literature. The different stages of the system are depicted in Fig. 3, while more details about the establishment of their associated LCI are explained in the following sections, and can be found in Tables S.6–S.11 of the Supplementary Materials.

2.5.3.1. Off-shore wind farm.
All phases of the life cycle should be taken into account when evaluating the environmental impact of the electricity produced by the offshore wind farm. Beginning with the production of the various parts, their installation, use, and maintenance, and concluding with the decommissioning and disposal of the buildings and machinery. Previous studies have performed the LCA of different off-shore wind turbine models, while also testing the effect of the operation and maintenance strategy [100,101], leading to different

results in terms of GWP. However, the results obtained are not dramatically different and therefore, for this assessment, a generic inventory is used to represent the production of electricity from an offshore wind turbine. This LCI is found in the Ecoinvent database, which is available in the SimaPro software, and comes under the name of "electricity production, wind, 1–3 MW turbine, offshore, GB". The database provides information of the high voltage electricity generated in 2012 at UK offshore wind farms connected to the grid. It covers infrastructure inputs as well as operating and maintenance costs. It is worth noting that the database does not account for the use of grid electricity during periods when the wind farm is not in operation. This is because the wind farm has been designed in a way that the electricity taken from the grid equals the electricity injected into it, thereby negating any environmental issues associated with the grid electricity.

2.5.3.2. Alkaline electrolyser. For this section, the LCI for the AE is taken from the work provided by Koj et al. [102]. This database provides a thorough inventory for the construction of a Zirfon alkaline electrolyser of 6 MW of capacity. At the same time, this database is combined with the comprehensive mass and energy balances produced in the current work based on [49]. All these data are accordingly arranged, normalized, and introduced in the software SimaPro, where a new inventory is created to represent AE construction and operation (maintenance is not considered due to the absence of data representing this activity). More details on this inventory could be found in Section S.4 of the Supplementary Materials. Concerning the AE's operation, no papers or studies have been found that analyse the effect of multi-functionality inherent to it, since an electrolyser not only produces hydrogen, but also by-products, such as oxygen and excess heat. Despite the opportunity of reducing emissions burden to the hydrogen (allocation) or gaining credits due to the displacement of industrial oxygen and heat for district heating production (system expansion), these options have not yet been considered due to some technical challenges and lack of technical and operational expertise, associated to the lack of commercial scale PtL plants [103]. In this sense, different scenarios for the allocation of the emissions in the AE operation are analysed, as explained in Table 6. The main assessment (AA1) assigns 100 % of the environmental impacts to hydrogen. The second approach (AA2) assumes an energy allocation, with no emissions attributed to oxygen, while the heat generated from the isothermal operation of the electrolyser is now considered a by-product. Finally, the third approach (AA3) considers both oxygen and district heating as by-products, by using exergy allocation.

2.5.3.3. Direct air capture. The inventories for the DAC technology is based on two studies found for the Climeworks technology [6,104]. Deutz et al. [6] and Terlouw et al. [104] provided for the first time complete LCA of a VTSA DAC unit at industrial scale, based on proprietary and confidential information provided by Climeworks, in which refers to the construction of the DAC unit. Despite the fact that the authors did not share this LCI, Terlouw et al. [104] provided a rough inventory based on freely accessible databases that could replicate their obtained findings. Consequently, these inventories were applied to represent the construction of the studied DAC technology. As for the operation, the LCI is also based on the data provided by [6,104]; however, some numbers are adjusted to reflect the energy and water integration of the DAC system, to the other sections of the plant.

2.5.3.4. Refinery plant. The inventory of the refinery plant is based on the generated mass and energy balances from Aspen Plus, which are normalized for 1 MJ (LHV based) of SAF. The inventory for the construction of the infrastructure is based on the existing inventory for "Chemical factory, organics {GLO}| market for | Cut-off, U" available in Ecoinvent.

2.5.3.5. Transport of jet fuel. The Ecoinvent database for "Kerosene {Europe without Switzerland}| market for kerosene | Cut-off, U" [105] is selected to represent this stage. This inventory includes information on the transport of the fuel from the process plant to the final consumer, which includes data for the operation of storage tanks, and the emissions attributable to the SAF's evaporation, as well as to the effluent treatment.

2.5.3.6. End use (combustion). Utilizing jet fuel in an airplane is the final phase of the life cycle. The emissions for the combustion of SAF are obtained from the Ecoinvent database for "Transport, passengers, aircraft, medium haul | Cut-off, U". Since SAF's chemical characteristics closely resemble those of jet fuel, this supposition is considered accurate [99]. In this stage, it is also important to mention that carbon neutrality [106] is assumed for the CO_2 emissions derived from combustion of SAF, since the main building block of the SAF is atmospheric CO_2.

2.5.4. Impact assessment: Global warming potential and water consumption

Among the midpoint impact categories available in SimaPro, the "Recipe 2016 midpoint (H)" is selected due to its popularity among LCA practitioners, as well as its ability to estimate GWP for a 100-year time horizon. Out of the 18 calculated environmental impacts, the GWP and water consumption are further discussed:

Global Warming Potential: This effect measures the infrared radiative force caused by GHG emissions, which are given as $kgCO_{2eq}$, and characterisation factors are used for gases other than CO_2. Since the SAF derives from CO_2 drawn from the atmosphere, it is believed that their combustion generate CO_2 with a characterization factor of zero. Water consumption: Water is an important resource in the production of hydrogen for the PtL plant. While being the main resource for the process of hydrogen generation, it is also used as a cooling utility. Understanding the water balance is important when it comes to economic and mainly environmental performances of the integrated PtL system. The water utilisation and consumption is accounted in every stage of the process, as mentioned in Section 2.2.6. However, the water utilisation of background LCI is detailed in the databases provided by Ecoinvent, alongside the results of Section 2.2.6 provide a better accounting of this resource which is as well calculated by ReCiPe Midpoint (H).

2.6. Sensitivity and uncertainty analysis for the TEA and LCA assessments

As shown in Table 2 for the TEA, the parameters linked to high uncertainty are modified. According to the classification of the AACE International, for low level of maturity plants, as in the case of the PtL process plant, the CAPEX of the refinery is changed between −30 % and +50 % [107]. Analyses of various tax and discount rates values and other significant economic characteristics are also conducted. The risk of investing in a specific project is correlated with the discount rate. For investments in PtL process plants, an optimistic discount rate of 8 % is suggested [108], whereas a pessimistic discount rate of 12 % is suggested. To reflect a scenario in which the PtL process might qualify for tax exemptions, the optimistic tax rate value is set at 0 %, while the higher value is set at 40 %. Supporting policies towards renewable

Table 2
Variables used for the sensitivity and uncertainty analyses of the TEA.

Parameter	Low Value	Nominal	High value	Unit
CO_2 cost	50	359	1000	£/tonne CO_2
H_2 cost	1	3.09	8	£/kg H_2
CAPEX refinery	40.63	58.04	87.06	MM£
Cost of wind electricity	0.030	0.060	0.09	£/kWh
Cost of network use	0	0.009	0.014	£/kWh
TAX rate	0.00	30.00	40.00	%
Discount rate	8.00	10.00	12.00	%

energy industries may subsidise the network cost for the grid electricity [83], and therefore a bandwidth between 0 to +50 % is considered for this parameter.

For the estimation of the MJSP, the TEA model requires inputs of CAPEX and OPEX estimations of the different sections of the integrated system. However, for ease of interpretation, the TEA model is modified for the sensitivity assessment and, instead of requiring individual CAPEX/OPEX of the CO_2 and H_2 production sections, the cost of capturing CO_2 and producing H_2 are the new inputs; in this way the readers can correlate costs with different technologies for capturing CO_2 and producing H_2. Table 2 shows the ranges of these costs using both an optimistic and pessimistic perspective:

The variables taken into account for the sensitivity analysis of the GWP are listed in Table 3. In order to find trustworthy values, the low, nominal, and high values for each parameter were evaluated in the current literature. Given that the system needs a lot of electricity, parameters related to electricity are essential. There are numerous studies that examine the carbon footprint of energy produced by wind; the NREL [101] developed a study that harmonised them, and this analysis took into account both the reported low and high values. Similar to this, several values for the stack efficiency of the AE were identified [51,109–111]; as a result, the low and high values from this review were taken into consideration. The expected reductions of the DAC energy requirements, as a result of the improvements in the Climeworks technology, are used as the low heat and power demands [6]. As there are no reported high-values for DAC energy consumption, a 50 % increase over the nominal values is assumed. Likewise, sorbent efficiency, which translates into the sorbent to capture the CO_2 mass ratio, is considered for this sensitivity analysis; for this, the Deutz et al. [6] study provides low, nominal, and high values for it. Finally, three different scenarios are analysed: 1) the UK grid is provided instead of the dedicated renewable energy source. 2) Energy allocation is used for the allocation of the products of the refinery (naphtha, diesel and jet fuel) and electrolyser (hydrogen and district heating); and 3) 'Excess oxygen, exergy allocation', where exergy allocation is used for the allocation of the products of the refinery (naphtha, diesel and jet fuel), as in the base scenario, however, there is an exergy allocation applied to the electrolyser as well (hydrogen, excess oxygen not used in the refinery, and district heating).

Due to the novelty of the 'PtL' concept, the different variables considered for the TEA and LCA assessment are associated with some degree of uncertainty regarding their real value, as reflected in Tables 2 and 4. In this sense, the uncertainty analysis is essential to showcase the effect of the uncertain variables on the final results. Thus, this analysis is performed for the MJSP and the GWP based on the same parameters considered for the sensitivity analysis, except for the GWP that uses the first four variables of Table 3. While the sensitivity analysis changes

Table 3
Variables used for the sensitivity and uncertainty analyses of the LCA.

	Value			References		
	Low	Nominal	High	Low	Nominal	High
Electricity carbon intensity (gCO₂/kWh)	7	15.25	22.5	[101]	*	[101]
Alkaline Stack efficiency (%)	58	68.81	72.82	[112]	[49]	[49]
Sorbent amount (g/kg CO₂)	3	7.5	11.25	[6]	[6]	–
DAC power requirement [MJ/kgCO₂ captured]	1.8	2.6	3.9	[6]	[6]	–
UK grid (gCO₂/kWh)	–	193.38	–	–	–	–
Excess oxygen, exergy allocation	–	–	–	–	–	–
Energy allocation	–	–	–	–	–	–

* Electricity, high voltage {GB}| electricity production, wind, 1–3 MW turbine, offshore | Cut-off, U.

Table 4
Literature review on technical performance of PtL studies for e-fuel production.

	Main Product	Carbon efficiency	Hydrogen efficiency	PtL efficiency
This study	Jet Fuel	88 %	39.16 %	28.06 %
Adelung et al. [10]	FT liquid fuels	88.00 %	28.00 %	38.70 %
Vidal-Vazquez et al. [8]	Oil and Wax	59.50 %	30.80 %	N/A
Vidal-Vazquez et al. [8]	Oil and Wax	94.00 %	32.00 %	47.00 %
Zang et al. [114]		45.53 %	24.35 %	52.20 %
König et al. [34]	FT liquid fuels	73.00 %	—	45 %
Hannula et al. [55]	FT liquid fuels	65 %–89 %	—	37 %–41 %
Hannula et al. [55]	FT liquid fuels	50 %–55 %	—	34 %–36 %
Marchese et al. [12]	FT liquid fuels	58.1 %–73.78 %	—	22.6 %–36.5 %

each parameter individually, a statistical method, such as the well-known Monte Carlo analysis allows the arbitrary modification of all of them at once. It is presumptively assumed that they all exhibit a triangular distribution. The MJSP and the GWP of the system is recalculated in 10,000 trials as part of the Monte Carlo analysis carried out in Matlab and the mean, median and standard deviation are calculated.

3. Results

3.1. Process modelling

This section presents the results of the mass and energy balances calculated using the various process models. Section S.5.1 of the Supplementary materials contains the results and validation of the FT unit. The DAC models estimate the amount of water that could be captured, and the results are used to explain the water integration and footprint. The process model created in Aspen Plus is critical for presenting mass and energy balances, which are then used for environmental and economic assessments. In addition, the water and energy integration are reflected in the mass and energy balances.

3.1.1. PTL process: Mass and energy balance

The mass and energy balances have been estimated, and Section S.5.2 of the supplementary materials presents them in detail for the main process streams and units. Overall, it is estimated that 13.3 tonne/h of CO_2 and 3.35 tonne/h of H_2 are required for the production of 0.88 tonne/h of naphtha, 2.52 tonne/h of jet fuel, and 0.81 tonne/h of diesel. Fig. 4 presents the carbon molar flow and distribution along the process and the products. Carbon is only lost to the atmosphere at the DAC unit and the purge gas, where 1.48 tonne/h and 0.29 tonne/h of CO_2 are emitted, respectively.

Based on these overall balances, and on the relations presented in Section 2.3, efficiencies such as carbon conversion, hydrogen conversion, and PtL, equal to 88.0 %, 39.16 %, and 25.6 %, respectively. Table 4 lists the findings from similar research that examined the synthesis of electrofuels using PtL/FT. It can be seen that the carbon conversion efficiency estimated for this study is in line with previous studies. High carbon efficiencies are highly linked to high CO_2 capture fractions and most studies assume capture of more than 90 %. The presence of appropriate recycling streams of the unreacted syngas to the synthesis sections is another crucial factor to take into account. In this sense, a combination of DAC with high CO_2 capture efficiency, as well as the existence of proper recycling streams (as in the present study), enhances the productivity of the products.

Due to the water synthesis that occurs at the RWGS and FT reactors, PtL systems have generally low hydrogen efficiency. One mole of water
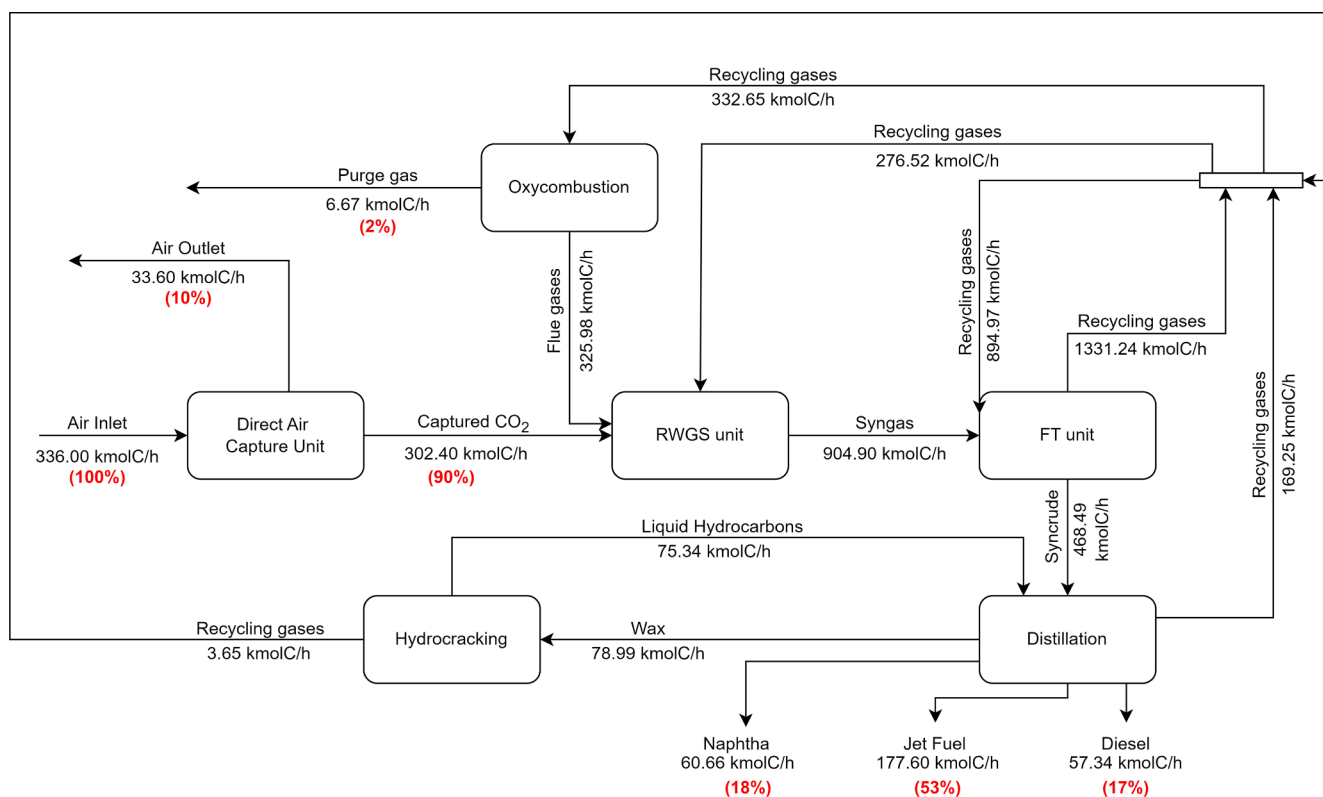
Fig. 4. The carbon mole flow of the investigated SAF route.

is synthesised for every mole of CO produced in the RWGS reactor, while at the FT reactor, the amount of produced water is greater (mole basis) than the hydrocarbons generated [113].The estimated hydrogen conversion efficiency of this study is higher than previous research and this is attributed to variations in the process configurations, such as the existence of several recycling streams as well as the employment of a comprehensive FT kinetic model.

Although the PtL efficiency is lower compared to other studies that are contrasted in Table 4, it is within the bounds reported in Marchese et al. [12]. The main reason for this is the utilisation of the kinetic approach for the FT reactor. As previously stated, the lumped kinetic model can predict the ASF model's deviations and predicts higher levels of CH_4 production of, which lead to lower production levels of liquid hydrocarbons and, thus, lower PtL efficiency.

3.1.2. DAC working capacities

Section S.5.3 of the supplementary materials illustrates, at atmospheric pressure, the influence of the RH over the CO_2 working capacity. These results [36] confirm the impact of temperature and relative humidity on the CO_2 working capacity: the latter increases with an increase in RH, with the impact being more pronounced at low temperatures. At the operating weather conditions that are taken from the data provided by Merra-2 for Teeside [42] (hourly temperature, pressure and relative humidity conditions for 2020), and considering temperature and pressure of desorption equal to 110 °C and 0.1 bar [36,115], the resulting working capacities for the CO_2 and the H_2O equal 2.82 molCO_2/kg and 9.61 molH_2O/kg of sorbent, respectively. In other words, for 1 kg of CO_2, 1.4 kg of water is produced. When compared with the literature, these results are in agreement with previous studies [36,115–117], for instance, DLR et al. found a value of 1 kg of extracted water per kg of captured CO_2 [117]. Based on the mass balance, which is presented in the Section S.5.2 of the Supplementary Materials, this water can cover 60 % of the electrolyser's water demand.

3.1.3. Heat and water integration

Fig. 5 illustrates the hot and cold streams taken into account for the Pinch Point analysis as a starting point for the heat integration. The streams that need cooling are shown in red on the diagram, whilst those needing heating are shown in blue. Since the heat released by the syngas combustion is integrated to the RWGS reactor and its inlet stream preheating, they are not taken into account for this diagram or the subsequent analysis. The hot and cold composite curves clearly show that the system's heat integration is a "threshold problem" rather than a "pinch point problem," which means that only one thermal utility is needed, and there is no pinch point temperature. As the process itself provides the necessary heating, no external hot utility is needed in this particular instance.

The streams that were taken into consideration for this heat integration, exchange heat when it is possible, but because the process requires more heat than it does cooling, the excess heat is used to produce steam at different qualities, as shown in Fig. S.4 of the Supplementary Materials. As a result, the cooling needs are met by the production of LP and HP steam, cooling water, and a refrigerant. There is no need to install an additional external heat source because the system itself completely meets the heating requirements. There is a synergy between the DAC unit and the process plant because the LP steam generated at the FT reactor is integrated with the DAC for the regeneration of the sorbent. Surplus LP and HP are produced at rates of 7.85 and 26.28 tonne/hr, respectively, which are considered as products with a positive economic input for the system.

The water integration is important for the hydrogen generation, which totally derives from water electrolysis. In total, 30.98 tonnes/h of water is required, from which 17.35 tonnes/h are potentially produced at the DAC unit, while the remaining requirement is considered to be provided by the process. The synthesis reactions occurring at the RWGS and the FT reactors are responsible of the production of 24.84 tonnes/h of water, from which 11.21 tonnes/h are sent to the electrolyser for the hydrogen generation. It is crucial to note that the water produced by the
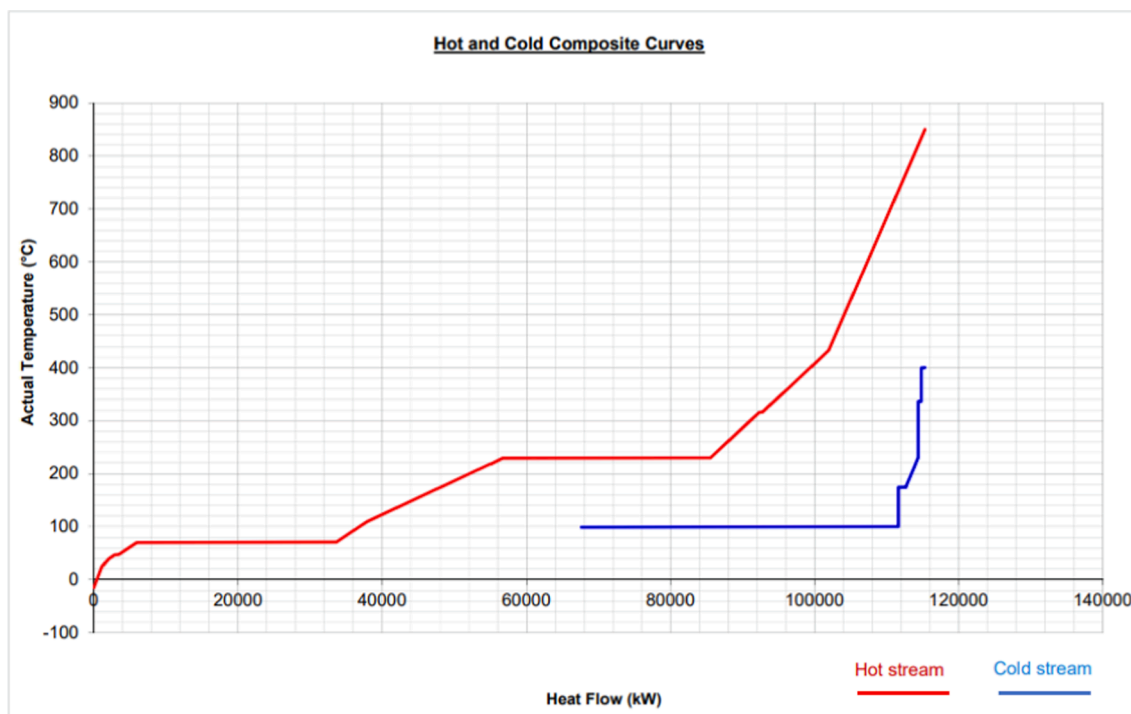
Fig. 5. The composite curves of the PtL system.

process may contain trace amounts of a variety of substances, including alcohols, ketones, aldehydes, carboxylic acids, and inorganic compounds [113]. As a result, it is crucial that industrial setups choose the best technology for treating the water. In terms of this study, a typical waste water treatment is taken into account. Although the selection of an adequate water treatment is outside the scope of this study, it is important to mention that if more rigorous purification techniques are needed, this could have an impact on the economic performance of the system.

3.1.4. Electricity requirements and wind farm electricity generation

The power demand for the various sections of the system are presented in Table 5. The dedicated off shore wind farm is designed in order to produce the requirements for the plant. Thus, 103 wind turbines can generate 199.69 MW based on the weather data and the wind farm's technical design. The annual hourly profile of energy generation (Fig. S.5 of the Supplementary Materials) reveals that there are times when the wind farm cannot produce the necessary energy. To tackle this, grid electricity is supplied to the system as part of the constant energy supply strategy explained in Section 2.2.2. In contrast, when the system generates more electricity than what is necessary, the excess is delivered to the grid. Overall, 660 MWh per year are exchanged between the wind farm and the grid.

3.2. Economic performance

Initially, the CAPEX of the system was evaluated, and it is estimated to be 331.55 MM£ (or 1.93 £/kg of SAF). The CAPEX breakdown of the process is 31 %, 18 % and 51 % for the electrolyser, the refinery plant

Table 5
The electricity demand of the integrated PtL system.

Process sections	Electricity demand [MW]
RefineryElectrolyserDirect Air Capture	5.57181.159.61
Overall electricity demand [MW]	
196.33	

Table 6
Description of different allocation methods.

Subsystem	Main and by-products	Products considered for the allocation method		
		Exergy allocation process plant, no allocation in the electrolyser (AA1)	Energy allocation (AA2)	Exergy allocation (AA3)
Electrolyser	Hydrogen	Yes	Yes	Yes
	Excess Oxygen	No	No	Yes
	District Heating	No	Yes	Yes
DAC	Carbon Dioxide	Yes	Yes	Yes
	Water	No	No	No
Process plant	Naphtha	Yes	Yes	Yes
	Diesel	Yes	Yes	Yes
	SAF	Yes	Yes	Yes
	Water	No	No	No

and the DAC respectively. The DAC unit is the dominating expense, and due to its early stage of development, the estimated DAC CAPEX is associated with significant uncertainty [118]. It is difficult to compare the predicted CAPEX with past PtL research because most of them used CO_2 capture costs as inputs for their economic assessment. A similar process configuration was studied by Comidy et al. [54], who found that the cost of the AE+RWGS reactor accounts for 59 % of the overall CAPEX. Similarly, Marchese et al. [88], analysed several scenarios for the production of FT-derived wax, finding CAPEX dominated by the cost of the DAC unit, which was based on a liquid sorbent (Carbon Engineering) technology.

The MJSP has been estimated as 5.16 £/kg of SAF (or 0.12 £/MJ). The process is OPEX intensive and the OPEX accounts for around 73 % of the MJSP, i.e., 3.76 £/kg; the OPEX breakdown is detailed in Fig. 6. This figure details the contribution of each component to the OPEX normalised per 1 kg of SAF. Based on these findings, it is possible to conclude that the cost of electricity (grid and wind-derived) accounts for the majority of the OPEX and, as a result, the MJSP. The annualised
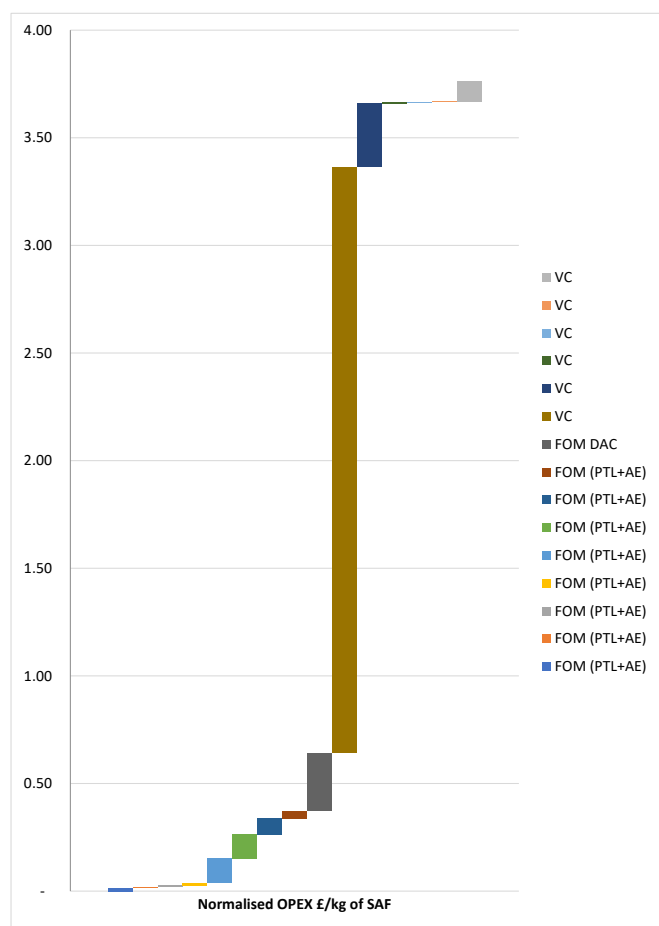
Fig. 6. The normalised OPEX of the investigated SAF route.

important point to discuss is that the studies that source their CO_2 requirements from a DAC unit, similar to this study, estimate larger minimum production costs for their PtL products, compared to other configurations with different CO_2 sources (e.g. concentrated sources); therefore, reducing CAPEX and OPEX costs of the various DAC technologies available in the market can play an important role on the reduction of production costs of e-fuels, alongside carbon credits that can be earned due to the utilisation of atmospheric CO_2.

3.2.1. Sensitivity analysis and economies of scale

The sensitivity of the calculated MJSP was assessed for the parameters listed in Table 2, with the outputs presented in Fig. 7; the blue and grey bars represent a reduction or increase in the baseline MJSP value, respectively. The largest variations are observed for the cost of producing H_2 and cost of capturing CO_2. Improvements in increasing the efficiency and decreasing the cost of the electrolyser is essential for cost reductions. In addition, lower electricity costs should be sought and ideally expected; in the UK, for example, low offshore wind electricity prices have already been attained in 2022 (0.037£/kWh) [119], which can be seen as an incentive for the development of PtL projects. The MJSP exhibits low sensitivity to the CAPEX of the refinery. Moreover, governments undoubtedly have a significant role to play in formulating tax rates that could help reduce the MJSP; however, even in the most optimistic scenarios, the MJSP never decreases to levels that could make SAF competitive with fossil-derived jet fuel. Therefore, to encourage the production and consumption of SAF, it is crucial for governments to offer carbon credits or other incentives.

The effect of economies of scale on the MJSP of the SAF, is shown in Fig. 8. The CAPEX of each section of the system was adjusted separately for the calculations at different capacities; for the refinery plant, an escalation factor of 0.65 was used; for the AE, a factor of 0.88 (calculated from reference [49]); and for the DAC, the learning rates methodology described in Section S.3 of the Supplementary Materials were applied. On the other hand, a linear adjustment to the capacity of the plant was assumed for all the raw materials, utilities, and products of the system, as detailed in Rojas et al. [63]. The MJSP can decrease by 15 % but the size of the plant should increase by approximately 5 times. When the PtL process is compared to a similar biomass to liquid (BtL) system for the production of SAF, the decline of the MSJP with the increase of the system's capacity is less steep than in the BtL system, as evidenced in the Rojas et al. [63] study. This is explained by the fact that PtL-derived SAF has been shown to be OPEX dependent, whereas BtL-derived SAF has a significant dependence on the CAPEX.

3.2.2. Uncertainty analysis

The Monte Carlo analysis yields mean and median MJSPs of 7.68 and 7.47 £/kg of SAF. The similarity of these values demonstrates the uniform distribution of the 10,000 datasets, and this is shown in Fig. 9. The MJSP could be located anywhere between 2.45 and 12.91 £/kg with a 95 % confidence. These findings highlight two points: first, the relatively high value of the standard deviation means that the distribution of the possible MJSP around the mean is very scattered due to the high level of uncertainty that is taken into account for the CO_2 and H_2 costs; and secondly, even in the most optimistic situation, the MJSP is never in a strong position against fossil jet fuel, which further supports the idea that incentives and carbon credits are necessary for PtL-derived SAF.

3.3. Environmental performance

The two primary environmental effects examined in the LCA are GWP and water footprint. The discussion of the selected allocation technique is crucial because the subsystems exhibit multifunctional behaviour. As explained in Section 2.5.2, the chosen allocation methods are based on energy or exergy content, due to the final utilisation of the products. The various factors that have been taken into account for each allocation method are shown in Table 6. The primary allocation
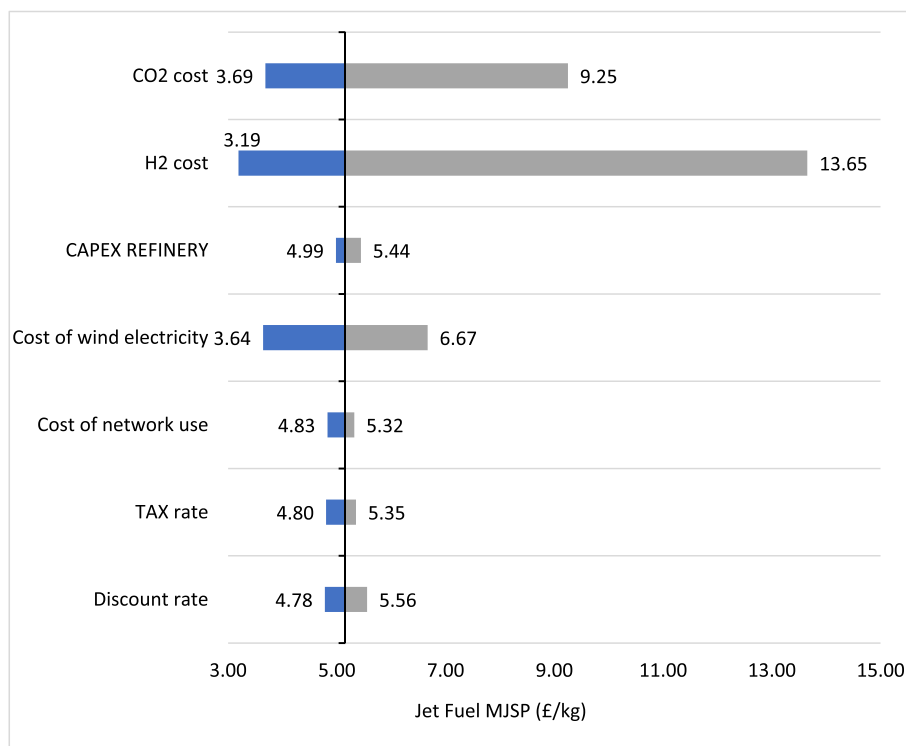
CAPEX is also a small proportion of the total MJSP, making the uncertainty created by certain equipment costs less significant when compared to the importance of the OPEX. Previous PtL based on FT studies found a variety of levelised costs of the analysed products, probably due to the differences in process configurations, plant capacities and equipment cost data; however, even under the most optimistic scenarios, all the estimated costs are much higher than the fossil-derived fuels. For example Hombach et al. [18] estimated a figure of 4.25 £/kg for the levelised cost of e-diesel in 2015, and a cost reduction to 3.37 £/kg for 2030, for DAC-derived CO_2 costs. Adelung et al. [13] calculated minimum selling costs ranging from 1.59 to 4.79 £/kg, for optimistic and pessimistic electrolysis-derived hydrogen scenarios, using CO_2 captured from a cement plant. In another study, Marchese et al. [88], estimated wax production costs ranging from 4.43 to 24.04 £/kg, based on liquid sorbent DAC technology for the capture of CO_2. Comidy et al. [54], assessed a system using nuclear energy and sea water acidification for CO_2 capture, and for the scenario operating with a dedicated nuclear power plant, the minimum production costs or aircraft carrier's fuel were found ranging from 2.52 to 3.28 £/L. Furthermore, existing research targeting jet fuel production is scarce, and for a similar process configuration as the one of this study, some reports were found in the open literature [15,19,21]. In the report of Batteiger et al. [19] a figure of 2.00–2.57 £/kg of SAF are presented for the near-term estimation of the MJSP. Long term (2050) estimations predict that the MJSP could drop to figures of 1.54–1.94 £/kg [15,19]. Similarly, Fasihi et al. [21] found values for the MJSP ranging between 1.20–1.43, 0.86–1.09 and 0.68–0.80 £/kg for 2030, 2040 and 2050, respectively.

The main conclusion of the analysed scenarios is that the economic performance of the SAF is attributed primarily to the high power requirements associated with green hydrogen generation. Another

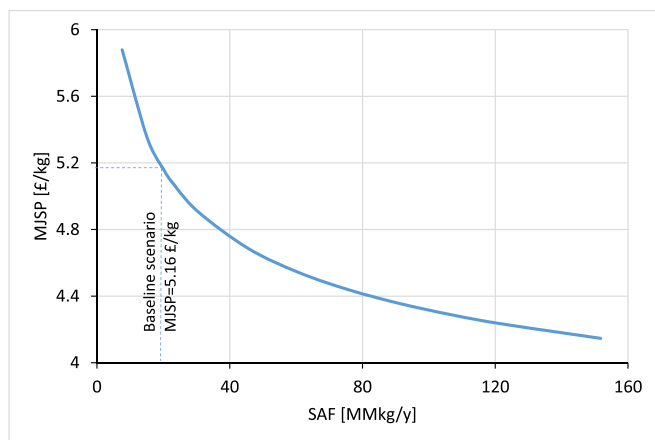**Fig. 7.** Sensitivity of the MJSP to various economic variables.

Fig. 8. Economies of scale for the of the investigated SAF route.

approach, for which the sensitivity and uncertainty analysis are developed, is the "Exergy allocation process plant, no allocation in the electrolyser," as a result of the facts disclosed in Section 2.5.3.2 about the by-products of the electrolyser. In the following sections, the GWP and water footprint results are widely analysed; however, for a more detailed overview of the other environmental impacts calculated by the ReciPe 2016 Midpoint (H) method, the reader is referred to Table S.12 of the Supplementary Materials.

3.3.1. Global warming potential

The GWP is estimated at $21.43 \, gCO_{2eq}/MJ$ and the largest contributor is the hydrogen production stage, as shown in Fig. 10. For more clarity about the role of the offshore-wind electricity, Fig. 11 provides more specific information about each stage of the WtWa LCA and how the offshore wind electricity contributed to them. Most of the emissions are due to the carbon footprint of the electricity. In this sense, strategies to even further reduce the GWP of the PtL-derived SAF could be

considered, such as improvement of the energy efficiency of the system and reduction of the carbon footprint of the electricity source (by improving construction, maintenance, and operation stages). On the other hand, it should be noted that the GWP performance of the SAF complies with the threshold emissions reduction set by the European Renewable Energy Directive II (RED II) [90], the Renewable Fuels Standard (RFS) [91], and the UK SAF mandate [28].

Some LCA studies have assessed the GWP of FT/PtL for liquid fuels synthesis [18,54,120], and some the specific scenario of jet fuel production [15,17,19,22]. The carbon footprint performance of SAF production was found as $13.88 \, gCO_{2eq}/MJ$, $5-10 \, gCO_{2eq}/MJ$ and $1 \, gCO_{2eq}/MJ$, by Falter et al. [17], Batteiger et al. [19], and Schmidt et al. [15], respectively. The GWP value estimated herein, i.e. $21.43 \, gCO_{2eq}/MJ$, is of the same order of magnitude, but still significantly higher. These discrepancies may be attributed to factors such as the choice of the DAC technology, the process configuration of the refinery (no FT off-gas recirculation), assumptions for the refinery's mass/energy balance (use of simplified models instead of detailed models), as well as the use of various energy sources to provide electricity. Further, recent studies such as Micheli et al. [22] display a value of $13.4 \, g \, CO_{2eq}/MJ$ for a similar system, while the Royal Society report [121] displays a range of $17-27 \, gCO_{2eq}/MJ$ for PtL SAF. It is important to point out that none of these studies or reports have examined synergies between the main components (CO_2 capture, H_2 production and refinery) of the PtL systems as we did in the current research such as the water and heat integration previously discussed.

3.3.2. Sensitivity analysis on the GWP

The sensitivity of the calculated GWP was assessed for the parameters listed in Table 3, with the outputs presented in Fig. 12, with the blue and grey bars representing a reduction or increase in the baseline GWP value. The GWP exhibits great sensitivity to the electricity carbon intensity. Furthermore, as shown in Fig. 12, increasing the energy efficiency of the AE and the DAC, which are the two largest electricity consumers of the system, barely affects the GWP. Some scenarios were evaluated by taking into account various allocation strategies or a
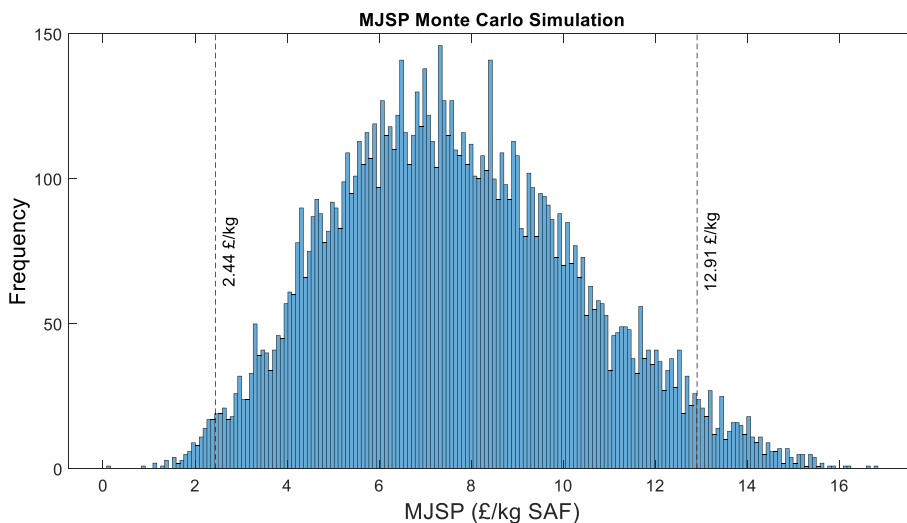
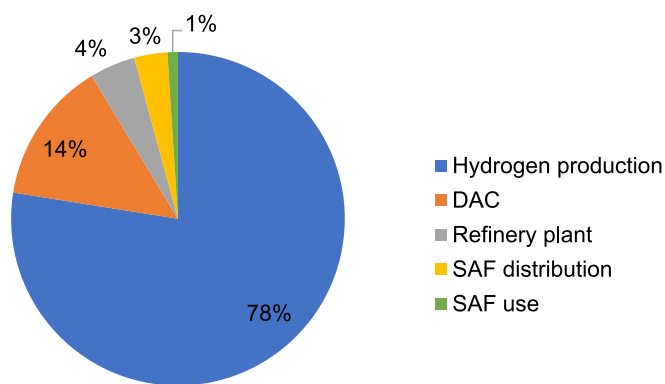**Fig. 9.** Uncertainty analysis of the MJSP.

Fig. 10. The breakdown of the GWP for each process stage.

different energy supply, such as electricity from the UK grid. Regarding the system's multi-functionality, the GWPs for the energy (AA2) and exergy allocation (AA3) decrease by 13.15 % and 7.59 %, respectively, when compared with the baseline allocation scenario (AA1). This decrease can be explained by the fact that AA2 and AA3 considered that the electrolyser-related emissions are distributed upstream among its by-products (oxygen, heat), reducing the burden on the H_2 and, consequently, the GWP of the final SAF. Nevertheless, it appears that the different allocation methods do not have a great effect on the GWP. The same cannot be said for the scenario using the current UK grid electricity mix. As it can be seen, using grid energy rather than a dedicated offshore wind farm increases the GWP by almost ten times. Based on these findings (except for the grid electricity scenario), the SAF synthesised under any low/high bounds of the examined parameters will always comply with the most stringent emissions reduction threshold (RED II).

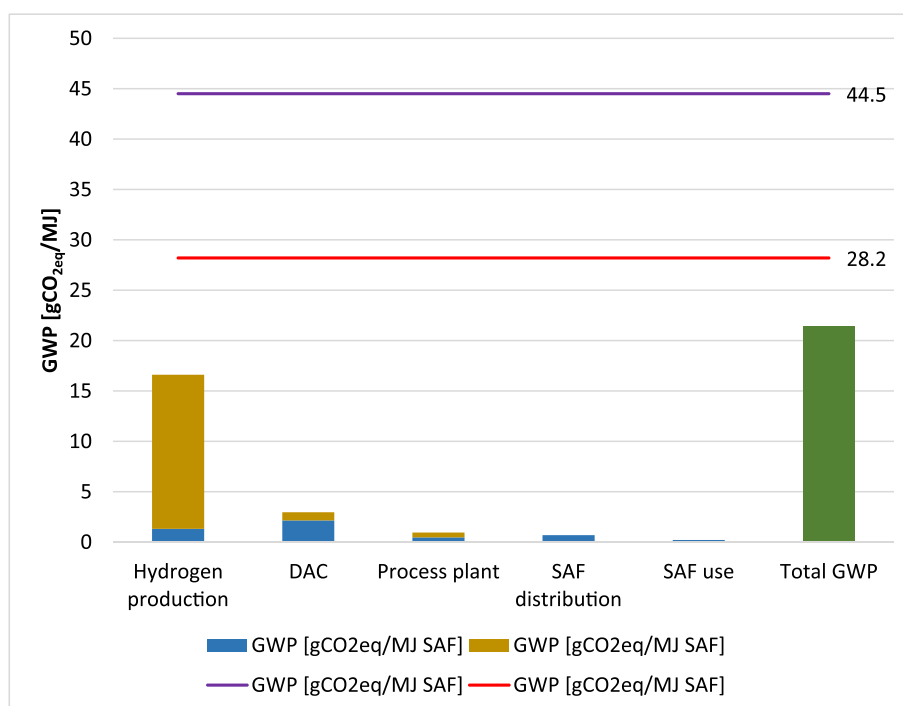Further, the sensitivity of the GWP is assessed for different electricity

Fig. 11. The contribution of electricity for each process stage, the overall GWP and comparison with existing sustainability standards.
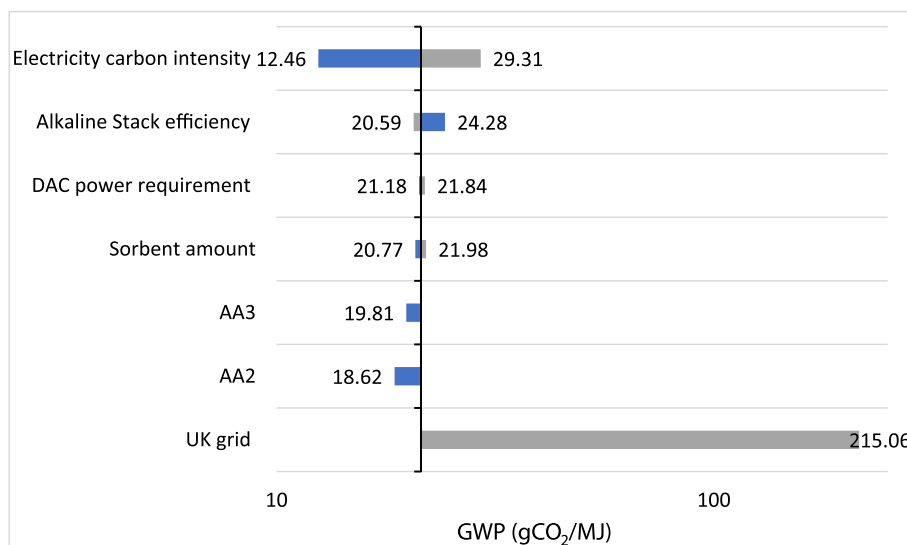
Fig. 12. Sensitivity analysis on the GWP, and scenario analysis for other allocation methods (AA1 and AA2) and UK grid electricity.

sources at different total power requirements as depicted in Fig. 12. The range for the carbon footprint of the electricity is chosen according to the existing options that are part of the UK grid [122,123]; however, because the carbon footprint of the fossil-derived sources is very high, only low GWP sources are included. The range for the electricity consumption is based on the efficiency ranges considered for the electrolyser and DAC; the electricity requirement of the refinery plant is assumed unchanged). The GWP potential is recalculated at different conditions as shown in Fig. 13. The horizontal lines represent the various electricity sources. Clearly, high carbon footprint electricity sources increase the GWP of the SAF. In the bottom of the diagram, Wind, Nuclear and Norwegian import (named in decreasing order) are able to produce SAF with GWP below the SAF mandate threshold at any system power consumption. Moreover, changes in the amount of required electricity does not have a big impact on the GWP, especially for low carbon footprint electricity sources. Thus, achieving low GWP SAF should rely in electricity sources such as wind or nuclear.

3.3.3. Uncertainty analysis on the GWP

Fig. 14 depicts the results for the Monte Carlo analysis on the GWP. Further the mean and median GWP values equal to 21.05 and 21.13 gCO_{2eq}/MJ of SAF, respectively. Their similarity is attributed to the symmetric probability distribution. The standard deviation equals 3.54 gCO_{2eq}/MJ which translates into a 95 % interval of confidence between 14.10 gCO_{2eq}/MJ to 28.00 gCO_{2eq}/MJ. Based on these results, it is clear that regardless of the uncertainty associated, the GWP of the WtWa study will always result in a SAF that complies with all the emissions reduction thresholds for sustainable aviation fuels. It is expected that the standard deviation will become smaller as the involved technologies become more mature.

3.3.4. Water footprint

It is worth noting that the global warming potential is just one aspect of the environmental impact of SAF production from PtL, and other factors such as water footprint and land use should also be considered.
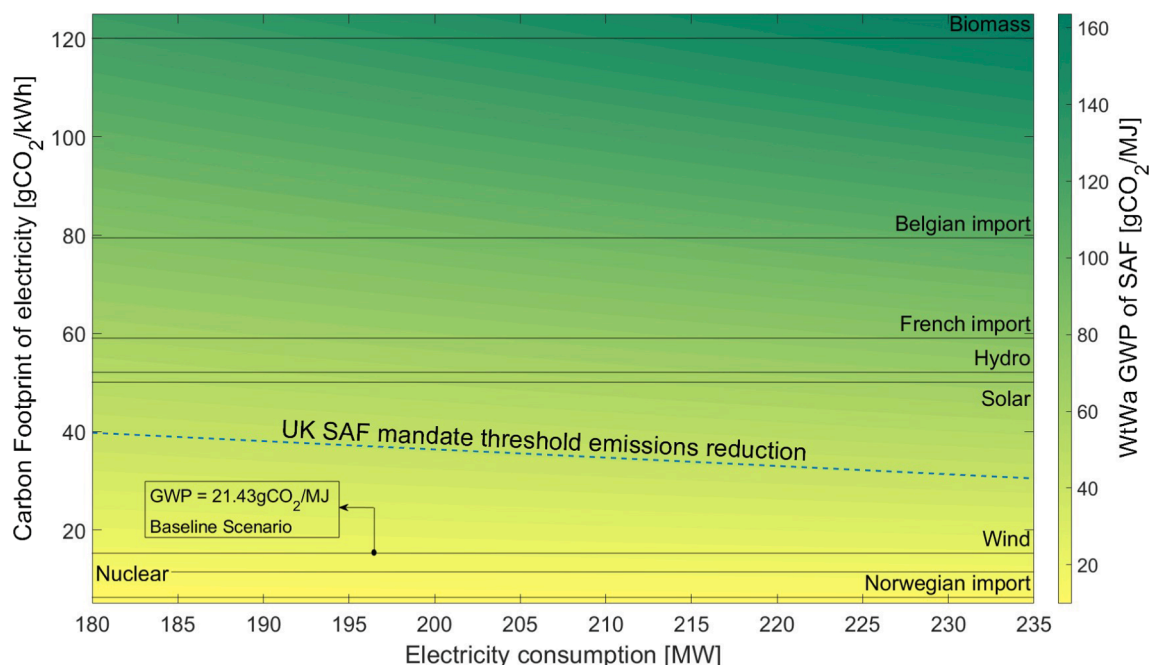

Fig. 13. The GWP of the WtWa life cycle of SAF for different electricity sources at different PtL electricity consumption.
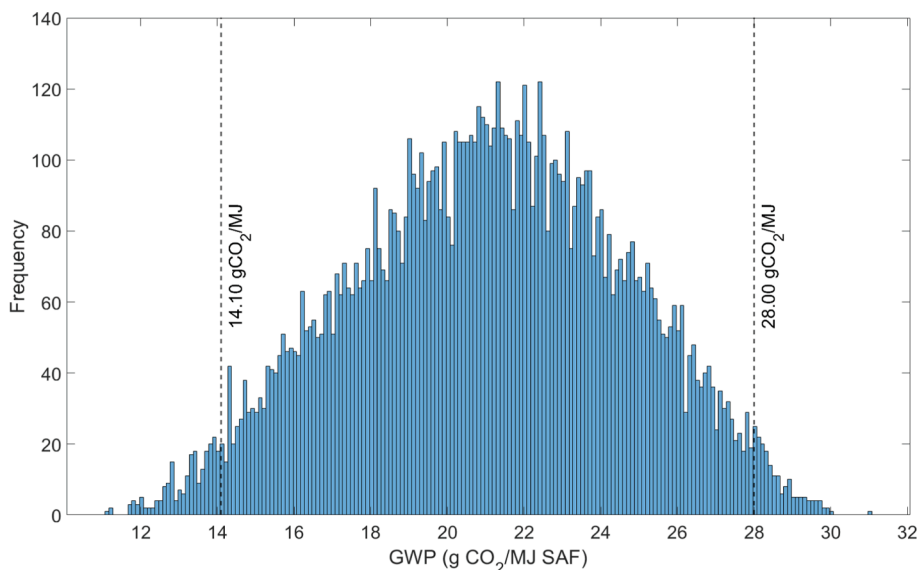
Fig. 14. Uncertainty analysis of the GWP.

However, reducing the water footprint of SAF production from PtL can help to reduce the overall environmental impact and improve the sustainability of aviation. The resulting water footprint for the analysed scenario equals 0.480 l/MJ of SAF and this is further detailed in Fig. 15.
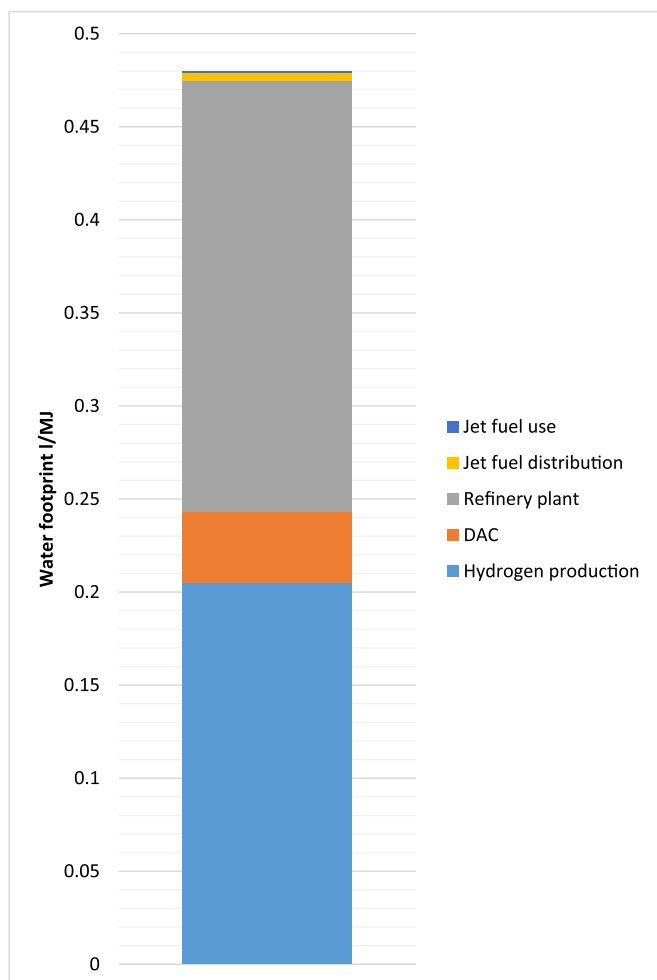

Fig. 15. The WtWa Water Footprint of the investigated SAF route.

It is obvious that the stage of hydrogen production accounts for almost 50 % of the overall water footprint of the WtWa analysis for SAF derived from PtL. Additionally, Fig. 16 show the precise impact of the different shares of the various steps for the three stages of the analysis that use the most water: the production of H_2, CO_2, and SAF. Fig. 16A shows the water footprint of H_2 production via AE, with negligible contributions from chemicals production (nitrogen, potassium hydroxide). The water requirement for the electrolysis reaction is covered by water produced in the DAC and the refinery, and thus not accounted for the water footprint calculations. It is thus evident that electricity generation has the greatest influence on the water footprint of hydrogen production, while the construction of the electrolyser is almost negligible.

Similarly to the AE, the DAC unit's water footprint does not account for the positive credit of water generated from the air because the electrolyser uses all of it, and therefore is not represented in Fig. 16B. In contrast to the generation of hydrogen, the phases of construction and chemical production (sorbent) are important for the water footprint calculations of this stage. The inventories used to represent the construction of the DAC unit, as well as the production of the sorbent, are taken from earlier research [6,104] that are available from Climeworks. It is crucial to note that the inventory provided for the construction phase was an adaptation of the original inventory, which was withheld from publication because it contained proprietary company data. Hence no details regarding the reliability of the water footprint of the adapted inventory are offered. In regards to the sorbent production, which is the main contributor to this stage, the inventory used for this analysis is derived from Terlouw et al. [104]. This inventory is a generic proxy that could represent any sorbent material. As a result of the importance of these two stages, the uncertainty associated with the water footprint of construction and sorbent production should be further investigated.

As depicted in Fig. 16C, it is clear that the water losses from the cooling water network have a great effect on the final water footprint. The design of the cooling water network estimates the amount of makeup water to replace cooling water losses; these losses will depend on the design operating parameters, as well as on the atmospheric conditions of the plant location. In this sense, an optimised design that targets heat integration, and/or the choice of air cooling system, could play an important role in the reduction of water footprint of this specific stage. Overall, it is found that the water footprint of SAF produced from PtL technology highly depends on the cooling water network design as well as on the water intensity of the electricity used to produce the fuel. Furthermore, the refinery stage benefits from a negative balance in the
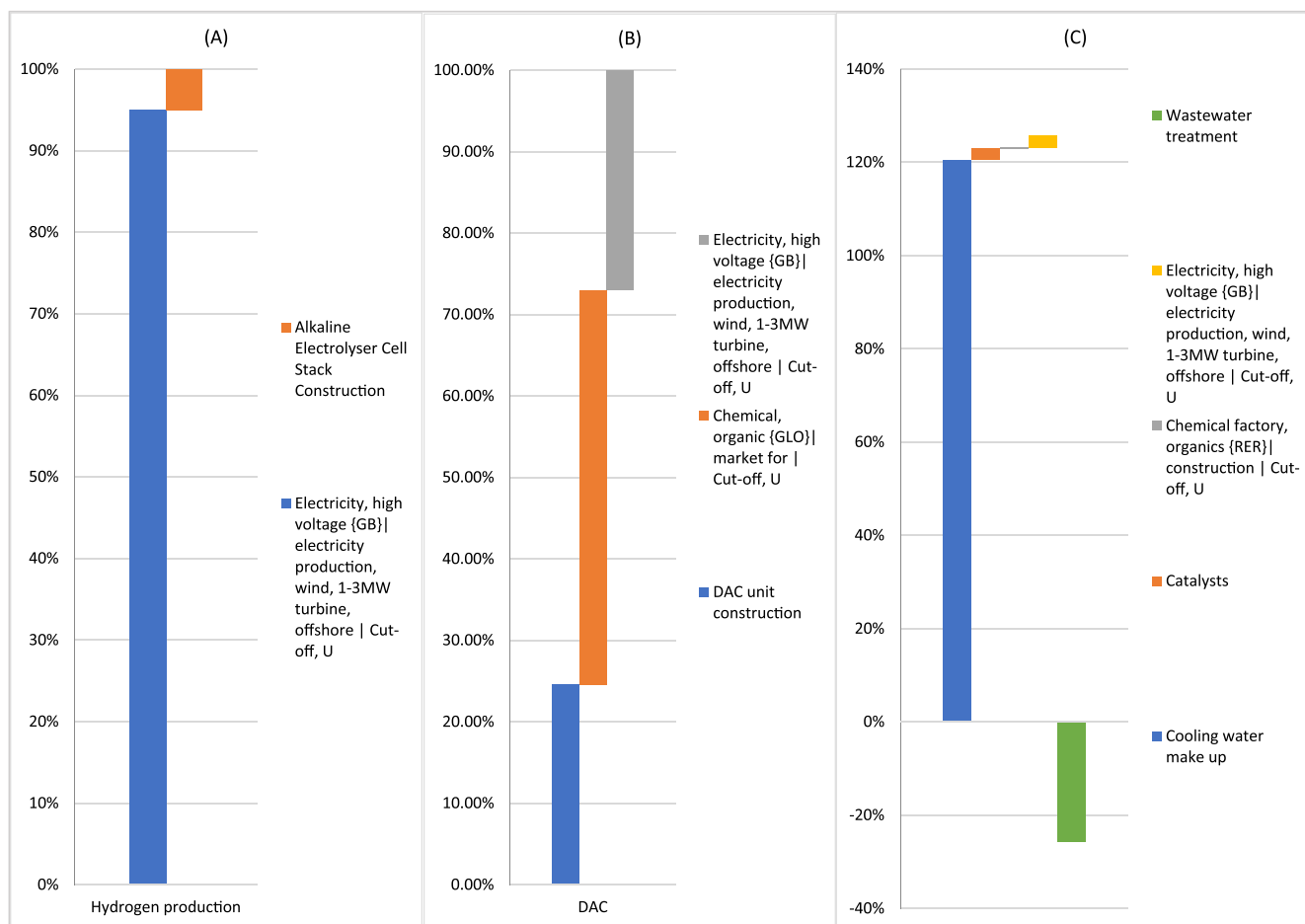
Fig. 16. The breakdown of the Water Footprint: A) hydrogen production stage. B) Direct Air Capture. C) Refinery plant.

final water footprint, since the amount of waste water goes to treatment, and after that, it can be utilized for other purposes such as agriculture.

According to a study published by Micheli et al. [22], the water footprint of SAF produced from PtL technology ranges from 6.19×10^{-3} to 0.182 l/MJ of SAF produced, when wind electricity is used, and the variation depends on the technology adopted for the DAC (High or low temperature) and the FT reactor (high or low temperature). For example, SAF produced using wind energy, LT DAC and LT FT reactor, has a water footprint of 0.113 l/MJ. The main difference with the value obtained by this work could be attributed that the former study

considered that the manufacturing and end of life of the associated equipment was negligible, while in this study it is seen that this affirmation is not exactly negligible for the DAC stage; another major difference is that the cooling water network was not considered, while this study shows that it has an important contribution, and therefore should be included in future LCA analysis of SAF studies. Other studies analysing the water footprint of SAF from PtL were elaborated by Batteiger et al. [19] and Schmidt et al. [15], who estimated 0.12 and 0.040 l/MJ of SAF, respectively; however, these analyses do not display the detailed assumptions behind the presented figures.
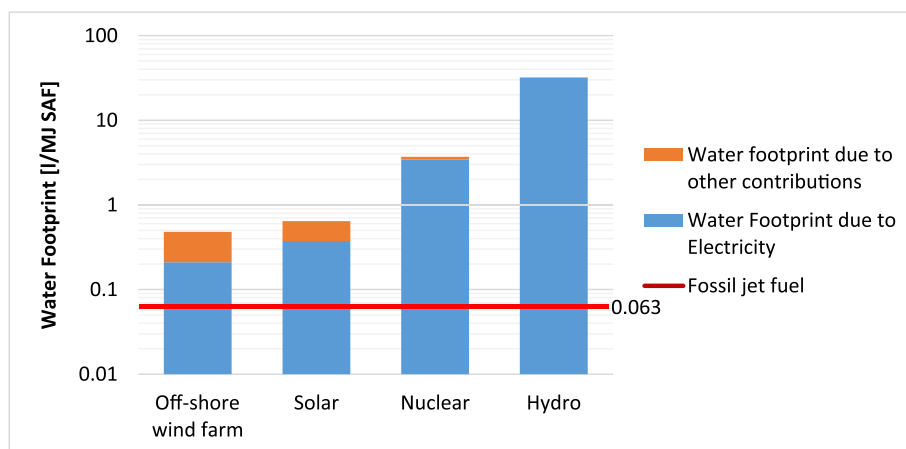

Fig. 17. Water footprint of the PtL-SAF when connected to different electricity sources.

Scenario analysis is performed considering some of the electricity sources used for the UK grid electricity. The water footprint of the considered sources was taken from Simapro-Ecoinvent Databases, as well as the water footprint of the fossil jet fuel. The results are depicted in Fig. 17. Among the represented energy sources, the off-shore wind farm shows a better performance compared to the other analysed sources, from which the hydropower has the biggest water footprint. It is evident that this environmental impact puts PtL-derived SAF in disadvantage against fossil jet fuel, regardless of the electricity source linked to the system. However, when compared against biomass-derived aviation fuels, the PtL-SAF has a water footprint 100 or 1000 times lower (as per the values displayed in the report of Schmidt et al. [15]).

3.4. Policy analysis: UK SAF mandate

It is evident that SAF achieves GHG emissions reduction, and that better environmental and economic performance could be achieved by increasing the production and use of SAF. As outlined by the ICAO [124], a range of policy options can be used to promote SAF, including financial incentives, regulations, mandates, and market-based mechanisms. Government subsidies and/or tax credits for companies producing SAF could help offset their expensive production, promoting their more widespread adoption. Similarly, carbon offset programs could be offered by governments or organizations, so companies can invest in SAF production projects in order to neutralize their environmental impact [125]. Moreover, the creation of guaranteed markets for SAF producers, through the establishment of mandates or targets, could drive investment and innovation to the industry.

The UK government has set a mandate for the use of sustainable aviation fuels (SAF) in commercial aviation. By 2030, all UK airlines must use fuel blends that contain a minimum of 10 % SAF, while this will be increased to 50 % by 2050. The mandate is a part of a broader government strategy to attain net-zero emissions by 2050 and to promote the growth of a sustainable aviation industry. The mandate includes a number of actions to aid in the creation and application of SAF, such as the establishment of a stakeholder engagement process, the development of a SAF clearinghouse to aid in the trading of SAF certificates, and the provision of financial incentives for SAF production and application [27,28].

The SAF certificate scheme is applied to simulate various scenarios and calculate the certificate price at which the SAF breaks-even with the fossil jet fuel (gate cost assumed at 0.56 £/kg [126]), for different CO_2

capture, and H_2 production costs. The number of certificates is estimated according to the second consultation of the SAF mandate [127]. Under this approach, the number of certificates is a function of the energy content of the produced SAF ($m \times LHV_i$) (Equation (26). However, to promote the use of SAF with larger GHG emissions savings, the number of certificates is also a function of the carbon intensity of the fuel. For the calculation of the carbon intensity factor (CI_{factor}) of the SAF (Equation (27), it is assumed that the average CI of SAF (CI_b) is 26.7 gCO_{2e}/MJ for a baseline scenario (which considers a SAF with a GWP reduction of 70 % compared to fossil jet fuel), that is compared with the emissions of fossil jet fuel (CI_F) which is taken as 89 gCO_{2e}/MJ [127]. The carbon intensity of the SAF, CI_{SAF}, is the estimated GWP, which is equal to 21.43 gCO_{2eq}/MJ.

$$Certificates = m \times LHV_i \times CI_{factor} \qquad (26)$$

$$CI_{factor} = \frac{CI_F - CI_{SAF}}{CI_F - CI_b} \qquad (27)$$

Fig. 18 illustrates the price at which the certificates must be purchased for SAF to break even the cost of conventional jet fuel for different H_2 production costs and CO_2 capture costs. For illustration purposes and to account for even the most unfeasible LCOH for blue and green hydrogen, the considered values take into account a cost range of 1–8 £/kg. A range of 30–1000 £/tonne is taken into account for the CO_2 capture cost to represent even the most expensive situation due to the low TRL of DAC technologies. Furthermore, Fig. S.6 of the Supplementary Materials present the same results for the certificate cost, but for the carbon impact factor calculated when no upstream emissions are considered for the electricity of the wind farm.

The calculated CI_{factor} is 1.08 and the annual production of SAF is 8.64E+8 MJ/year. The investigated process is eligible for 9.37E+8 certificates per year. According to this figure, the cost of the SAF certificate should be 0.10 £ for the baseline scenario to break-even. Further, the hydrogen produced through biomass gasification with CCU at two distinct scales is presented, along with hydrogen produced by an AE electrolyser from dedicated wind farms and electricity curtailment, at the estimated 2030 cost by BEIS [128]. It is evident that better economic performance is achieved when using hydrogen produced from biomass or curtailed energy. However, limited availability of biomass and of curtailed electricity pose challenges in scaling-up SAF production technologies.
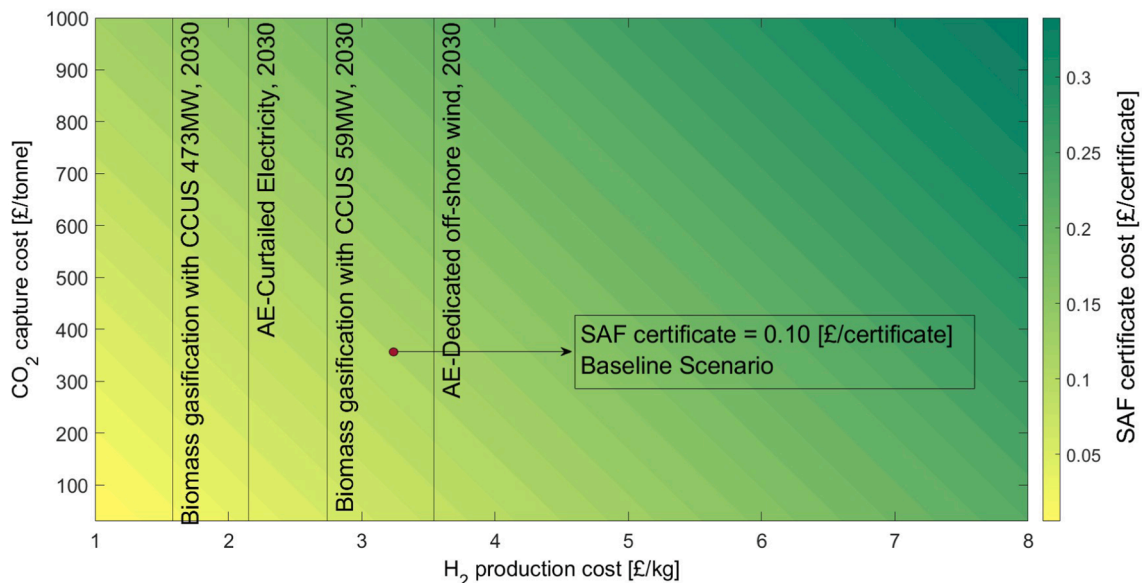

Fig. 18. The SAF certificate cost for the MJSP to break-even with fossil jet fuel cost (0.56£/kg) for different CO_2 capture and H_2 production costs.

4. Conclusions

The aviation industry has set an action plan, in which the development and use of SAF could have the largest impact on decarbonising the sector. The development of such SAF alternatives face technical, economic and environmental issues. Therefore, the development of integrated techno-economic and environmental assessments can provide a better overview on the performance metrics and identify actions that can improve and accelerate their deployment.

Within this context, this research has jointly examined the economic and environmental performance of SAF production through the PtL pathway in the UK. The system has been designed to maximize the potential benefits of integrating its various components. For example, incorporating the LT DAC unit presents an opportunity to integrate heat from other parts of the process, such as the heat released by the FT reactor. Additionally, the DAC unit produces water and this has been fed to the electrolyser. The economic and environmental evaluations provided significant insights that can be compared to fossil jet fuel. Further, a policy analysis explored ways to support the development of sustainable aviation fuel (SAF). The key findings of these various evaluations can be summarized as follows:

1. The process has a carbon conversion efficiency of 0.88, with PtL and hydrogen conversion efficiencies of 0.26 and 0.39, respectively. Despite modelling efforts to demonstrate this process configuration, there are still several sources of uncertainty, particularly regarding process design. These include the operation of the RWGS reactor, recycling streams to both RWGS and FT reactors, and operating conditions for different sections of the process. As more demonstration and pilot plants become operational, the uncertainties related to these values will decrease.

2. The energy balances indicate that the refinery plant has a lower energy demand compared to the AE and DAC operations. Although the off-shore wind farm has been shown to be a reliable dedicated energy source, ensuring a stable energy supply to the system will require strategies such as utilizing the grid as a virtual storage or designing an effective storage system.

3. The economic evaluation indicates that the cost of SAF produced by this pathway is not competitive with fossil jet fuel. The calculated MJSP stands at 5.16 £/kg and is highly sensitive to electricity and DAC costs. Therefore, technical and economic improvements in CO_2 and H_2 production technologies could lead to cost reductions in MJSP. Lower electricity prices or consumption result in better economic performance. Economies of scale demonstrate that increasing production capacity leads to cost reductions, but not as much as for biomass scenarios, since the PtL system is highly dependent on OPEX. However, it's worth noting that scaling up the PtL system is not limited by feedstock supply and has less location restrictions.

4. The life cycle assessment (LCA) of the system has shown that the global warming potential (GWP) of the SAF produced through this pathway is lower than that of fossil jet fuel and it can meet existing aviation emissions reduction targets, such as the UK SAF mandate. If the source of electricity is an off-shore wind farm (base case scenario), the GWP of the PtL system is 21.43 gCO_{2eq}/MJ. Moreover, the GWP is sensitive to the carbon footprint of the electricity, indicating its dependence on the energy source.

5. The water footprint of the PtL system is 0.48 l/MJ of SAF and is highly dependent on the water footprint of electricity generation and cooling water requirements. Therefore, a combination of system energy efficiency improvements and an optimal design of the cooling water system are essential for reducing the water consumption. Understanding the appropriate treatment of water synthesized in the PtL process plant could enable its use in an operating facility. Furthermore, it is important to highlight that the water footprint of PtL-SAF is higher than conventional fossil jet fuel. Nevertheless, compared to other SAF alternatives like biomass-derived fuels, the water footprint of PtL-SAF is significantly lower.

6. The Monte Carlo analysis of the MJSP revealed that it will always remain higher than the gate price of the conventional jet fuel. Therefore, more efforts and government economic incentives are necessary for these fuels to be widely adopted by the aviation industry. On the other hand, for the GWP, the uncertainty analysis showed that the SAF GWP will remain lower than the established UK SAF mandate threshold and other existing thresholds such as the RED II, or the RFS.

7. A policy analysis indicated that the SAF mandate certificate cost should be between 0.009 and 0.35 £/certificate depending on the CO_2 capture and H_2 production costs. For the base case scenario, the SAF mandate certificate should be equal to 0.10 £/certificate of SAF.

These conclusions are part of the growing body of research on power to liquids process configurations, with a particular focus on creating sustainable aviation fuels. It is pivotal that more demonstration and pilot plants should become operational, so that the uncertainties related to the technical, economic and environmental metrics will decrease. Based on the assumptions made in this study, it has been demonstrated that the Power to liquids has the potential to greatly decrease greenhouse gas emissions and thereby aiding the decarbonisation of the aviation industry. However, supporting policies are needed for further development and eventually deployment at large scale. Further research and data gathering for pilot/demo plants will support future investigations and applications.

CRediT authorship contribution statement

Maria Fernanda Rojas-Michaga: Conceptualization, Formal analysis, Methodology, Software, Validation, Writing – original draft. **Stavros Michailos:** Conceptualization, Methodology, Software, Investigation, Validation, Writing – review & editing. **Evelyn Cardozo:** Methodology, Software, Writing – review & editing. **Muhammad Akram:** Methodology, Validation, Writing – review & editing. **Kevin J. Hughes:** Resources, Supervision, Writing – review & editing. **Derek Ingham:** Project administration, Resources, Supervision, Writing – review & editing. **Mohamed Pourkashanian:** Resources, Supervision, Writing – review & editing.

Declaration of Competing Interest

The authors declare that they have no known competing financial interests or personal relationships that could have appeared to influence the work reported in this paper.

Appendix A. Supplementary material

Supplementary data to this article can be found online at https://doi.org/10.1016/j.enconman.2023.117427.

References

[1] European Environmental Agency, EASA, and EUROCONTROL. European aviation environmental report 2019; 2019. doi: 10.20289/eüzfd.59424.
[2] Chuck CJ. Biofuels for aviation: feedstocks, technology and implementation; 2016. doi: 10.1017/CBO9781107415324.004.

[3] Stratton RW, Wong HM, Hileman JI. Life cycle greenhouse gas emissions from alternative jet fuels; 2010.

[4] Schmidt P, Batteiger V, Roth A, Weindorf W. Power-to-liquids as renewable fuel option for aviation: a review. 2018;1:127–40. doi: 10.1002/cite.201700129.

[5] Yu Q, Brilman DWF. Design strategy for CO2 adsorption from ambient air using a supported amine based sorbent in a fixed bed reactor. Energy Proc 2017;114 (November 2016):6102–14. https://doi.org/10.1016/j.egypro.2017.03.1747.

[6] Deutz S, Bardow A. Life-cycle assessment of an industrial direct air capture process based on temperature–vacuum swing adsorption. Nat Energy 2021;6(2): 203–13. https://doi.org/10.1038/s41560-020-00771-9.

[7] Schäppi R, Rutz D, Dähler F, Muroyama A, Haueter P, Lilliestam J, et al. Drop-in fuels from sunlight and air. Nature 2022;601(7891):63–8. https://doi.org/10.1038/s41586-021-04174-y.

[8] Vidal F, Koponen J, Ruuskanen V, Bajamundi C, Kosonen A, Simell P, et al. Power-to-X technology using renewable electricity and carbon dioxide from ambient air: SOLETAIR proof-of-concept and improved process concept. J CO2 Util 2018;28(September):235–46. https://doi.org/10.1016/j.jcou.2018.09.026.

[9] Kaiser P, Jess A. Modeling of multitubular reactors for iron- and cobalt-catalyzed Fischer-Tropsch syntheses for application in a power-to-liquid process. Energ Technol 2014;2(5):486–97. https://doi.org/10.1002/ente.201300189.

[10] Adelung S, Maier S, Dietrich RU. Impact of the reverse water-gas shift operating conditions on the Power-to-Liquid process efficiency. Sustainable Energy Technol Assess 2021;43(November 2020):100897. https://doi.org/10.1016/j.seta.2020.100897.

[11] Marchese M, Giglio E, Santarelli M, Lanzini A. Energy performance of Power-to-Liquid applications integrating biogas upgrading, reverse water gas shift, solid oxide electrolysis and Fischer-Tropsch technologies. Energy Convers Manag 2020; 6(January):100041. https://doi.org/10.1016/j.ecmx.2020.100041.

[12] Marchese M, Buffo G, Santarelli M, Lanzini A. CO2from direct air capture as carbon feedstock for Fischer-Tropsch chemicals and fuels: energy and economic analysis. J CO2 Util 2021;46:101487. https://doi.org/10.1016/j.jcou.2021.101487.

[13] Adelung S, Dietrich R-U. Impact of the reverse water-gas shift operating conditions on the Power-to-Liquid fuel production cost. Fuel 2022;317:123440. https://doi.org/10.1016/j.fuel.2022.123440.

[14] Dietrich RU, Albrecht FG, Maier S, König DH, Estelmann S, Adelung S, et al. Cost calculations for three different approaches of biofuel production using biomass, electricity and CO2. Biomass Bioenergy 2018;111:165–73. https://doi.org/10.1016/j.biombioe.2017.07.006.

[15] Schmidt P, Weindorf W. Power-to-liquids: potentials and perspectives for the future supply of renewable aviation fuel. Dessau-Roßlau 2016;September:1–36 [Online]. Available: https://www.umweltbundesamt.de/en/publikationen/power-to-liquids-potential-perspectives-for-the.

[16] van der Giesen C, Kleijn R, Kramer GJ. Energy and climate impacts of producing synthetic hydrocarbon fuels from CO2. Environ Sci Technol 2014;48(12): 7111–21. https://doi.org/10.1021/es500191g.

[17] Falter C, Batteiger V, Sizmann A. Climate impact and economic feasibility of solar thermochemical jet fuel production. Environ Sci Technol 2016;50:470–7. https://doi.org/10.1021/acs.est.5b03515.

[18] Heidgen K, Maas H, Hombach LE, Dor L, Wallington TJ, Walther G. Economic and environmental assessment of current (2015) and future (2030) use of E-fuels in light-duty vehicles in Germany. 2019;207:153–62. doi: 10.1016/j.jclepro.2018.09.261.

[19] Batteiger V, Ebner K, Habersetzer A, Moser L, Schmidt P, Weindorf W, et al. Power-to-liquids – a scalable and sustainable fuel supply perspective for aviation; 2022. [Online]. Available: https://www.umweltbundesamt.de/en/publications.

[20] Schmidt PR, Zittel W, Weindorf W, Raksha T. Empowering a sustainable mobility future with zero emission fuels from renewable electricity; 2016. p. 203.

[21] Fasihi M, Solomon OA. E-kerosene for commercial aviation from green hydrogen and CO2 from direct air capture – volumes Cost 2022;September.

[22] Micheli M, Moore D, Bach V, Finkbeiner M. Life-cycle assessment of power-to-liquid kerosene produced from renewable electricity and CO2 from direct air capture in germany. Sustainability (Switzerland) 2022;14(17). https://doi.org/10.3390/su141710658.

[23] Drechsler C, Agar DW. Intensified integrated direct air capture - power-to-gas process based on H2O and CO2 from ambient air. Appl Energy 2020;273(April): 115076. https://doi.org/10.1016/j.apenergy.2020.115076.

[24] Surgenor C. Europe's first power-to-liquid demo plant in Norway plans renewable aviation fuel production in 2023. One (Only Natural Energy); 2020. https://www.onlynaturalenergy.com/europes-first-power-to-liquid-demo-plant-in-norway-plans-renewable-aviation-fuel-production-in-2023/(accessed Jan. 10, 2022).

[25] Die Bundesregierung. PtL-Roadmap: Initiativen der Bundeslander; 2021.

[26] Muller N, King N. Aviation: Germany opens world's first plant for clean jet fuel. DW; 2021. https://www.dw.com/en/sustainable-aviation-fuel-power-to-liquid/a-59398405 (accessed Jan. 10, 2022).

[27] Department For Transport. Sustainable aviation fuels mandate: a consultation on reducing the greenhouse gas emissions of A consultation on reducing the greenhouse gas emissions of aviation fuels in the UK greenhouse gas emissions of aviation fuels in the UK; July, 2021 [Online]. Available: https://assets.publishing.service.gov.uk/government/uploads/system/uploads/attachment_data/file/1005382/sustainable-aviation-fuels-mandate-consultation-on-reducing-the-greenhouse-gas-emissions-of-aviation-fuels-in-the-uk.pdf.

[28] Department for Transport. Sustainable aviation fuels mandate: summary of consultation responses and government response; July 2022, 2022.

[29] Department for Transport. Jet zero consultation; 2021. [Online]. Available: https://assets.publishing.service.gov.uk/government/uploads/system/uploads/attachment_data/file/1002716/jet-zero-consultation-a-consultation-on-our-strategy-for-net-zero-aviation.pdf.

[30] Grahn M, Malmgren E, Korberg AD, Taljegard M, Anderson JE. Review of electrofuel feasibility — cost and environmental impact Progress in Energy. Prog Chem Org Nat Prod 2022.

[31] Goodman G, Martin V. Wind powered electricity in the UK. Offshore Wind Outlook 2019, May 2020; 2019. p. 1 [Online]. Available: www.iea.org/reports/offshore-wind-outlook-2019 %0Ahttps://assets.publishing.service.gov.uk/government/uploads/system/uploads/attachment_data/file/875384/Wind_powered_electricity_in_the_UK.pdf.

[32] Onshore vs offshore wind energy: what's the difference? | National Grid Group. https://www.nationalgrid.com/stories/energy-explained/onshore-vs-offshore-wind-energy (accessed Apr. 12, 2022).

[33] Department for Transport. Low carbon fuels strategy Call for ideas; 2022. Accessed: Apr. 24, 2023. [Online]. Available: https://www.gov.uk/government/consultations/low-carbon-fuel-strategy-call-for-ideas.

[34] König DH, Freiberg M, Dietrich RU, Wörner A. Techno-economic study of the storage of fluctuating renewable energy in liquid hydrocarbons. Fuel 2015;159: 289–97. https://doi.org/10.1016/j.fuel.2015.06.085.

[35] Marchese M, Chesta S, Santarelli M, Lanzini A. Techno-economic feasibility of a biomass-to-X plant: Fischer-Tropsch wax synthesis from digestate gasification. Energy 2021;228:120581. https://doi.org/10.1016/j.energy.2021.120581.

[36] Sabatino F, Grimm A, Gallucci F, van Sint Annaland M, Kramer GJ, Gazzani M. A comparative energy and costs assessment and optimization for direct air capture technologies. Joule 2021;5(8):2047–76. https://doi.org/10.1016/j.joule.2021.05.023.

[37] Fasihi M, Olga E, Breyer C. Techno-economic assessment of CO 2 direct air capture plants. J Clean Prod 2019;224:957–80. https://doi.org/10.1016/j.jclepro.2019.03.086.

[38] McQueen N, Gomes KV, McCormick C, Blumanthal K, Pisciotta M, Wilcox J. A review of direct air capture (DAC): scaling up commercial technologies and innovating for the future. Prog Energy 2021;3(3):032001. https://doi.org/10.1088/2516-1083/abf1ce.

[39] Beuttler C, Charles L, Wurzbacher J. The role of direct air capture in mitigation of anthropogenic greenhouse gas emissions; 2019. p. 1–7. doi: 10.3389/fclim.2019.00010.

[40] Gebald C. Development of amine-functionalized adsorbent for carbon dioxide capture from atmospheric air. ETH Zürich, no. 21853; 2014. p. 1–133 [Online]. Available: https://www.research-collection.ethz.ch/handle/20.500.11850/97310.

[41] Wurzbacher JA, Gebald C, Brunner S, Steinfeld A. Heat and mass transfer of temperature-vacuum swing desorption for CO2 capture from air. Chem Eng J 2016;283:1329–38. https://doi.org/10.1016/j.cej.2015.08.035.

[42] MERRA-2. https://gmao.gsfc.nasa.gov/reanalysis/MERRA-2/(accessed Aug. 29, 2022).

[43] Pacific Green. Green hydrogen: why batteries are a key part of the picture. https://www.pacificgreen-energystorage.com/articles/green-hydrogen-why-batteries-are-key-part-picture (accessed Jun. 09, 2022).

[44] Tebibel H. Methodology for multi-objective optimization of wind turbine/battery/electrolyzer system for decentralized clean hydrogen production using an adapted power management strategy for low wind speed conditions. Energy Convers Manag 2021;238:114125. https://doi.org/10.1016/j.enconman.2021.114125.

[45] Olateju B, Kumar A, Secanell M. A techno-economic assessment of large scale wind-hydrogen production with energy storage in Western Canada. Int J Hydrogen Energy 2016;41(21):8755–76. https://doi.org/10.1016/j.ijhydene.2016.03.177.

[46] Gökçek M, Kale C. Optimal design of a Hydrogen Refuelling Station (HRFS) powered by Hybrid Power System. Energy Convers Manag 2018;161(February): 215–24. https://doi.org/10.1016/j.enconman.2018.02.007.

[47] Ursúa A, Barrios EL, Pascual J, San Martín I, Sanchis P. Integration of commercial alkaline water electrolysers with renewable energies: limitations and improvements. Int J Hydrogen Energy 2016;41(30):12852–61. https://doi.org/10.1016/j.ijhydene.2016.06.071.

[48] García Clúa JG, Mantz RJ, De Battista H. Optimal sizing of a grid-assisted wind-hydrogen system. Energy Convers Manag Jun 2018;166:402–8. https://doi.org/10.1016/j.enconman.2018.04.047.

[49] Holst M, Aschbrenner S, Smolinka T, Voglstätter C, Grimm G. Cost forecast for low temperature electrolysis - technology driven bottom-up prognosis for PEM and alkaline water electrolysis systems; 2021. p. 79.

[50] Simon AJ, Daily W, White RG. Hydrogen and water: an engineering, economic and environmental analysis; 2010.

[51] Pietra A, Gianni M, Zuliani N, Malabotti S, Taccani R. Experimental characterization of an alkaline electrolyser and a compression system for hydrogen production and storage. Energies (Basel) 2021;14(17):1–17. https://doi.org/10.3390/en14175347.

[52] Jang D, Cho HS, Kang S. Numerical modeling and analysis of the effect of pressure on the performance of an alkaline water electrolysis system. Appl Energy 2021; vol. 287, no. January:116554. https://doi.org/10.1016/j.apenergy.2021.116554.

[53] Aspen Technology Inc. and Aspen Plus V 8.4. Aspen physical property system: physical property methods. Methods 2013:1–234. [Online]. Available: http://profsite.um.ac.ir/~fanaei/_private/Property Methods 8_4.pdf.

[54] Comidy LJF, Staples MD, Barrett SRH. Technical, economic, and environmental assessment of liquid fuel production on aircraft carriers. Appl Energy 2019;256 (June):113810. https://doi.org/10.1016/j.apenergy.2019.113810.

[55] Hannula I, Kaisalo N, Simell P. Preparation of synthesis gas from CO2 for Fischer-Tropsch synthesis—comparison of alternative process configurations. C—J Carbon Res 2020;6(3):55. https://doi.org/10.3390/c6030055.

[56] Wolf A, Kern C, Jess A. Renewable synthesis-gas-production - do hydrocarbons in the reactant flow of the reverse water-gas shift reaction cause coke formation? DGMK Tagungsbericht 2013;2013(2):215–21.

[57] Repasky JM, Zeller RL III. WO2021062384A1; 2021.

[58] dos Santos RG, Alencar AC. Biomass-derived syngas production via gasification process and its catalytic conversion into fuels by Fischer Tropsch synthesis: a review. Int J Hydrogen Energy 2019;45:1–19. https://doi.org/10.1016/j.ijhydene.2019.07.133.

[59] Ail SS, Dasappa S. Biomass to liquid transportation fuel via Fischer Tropsch synthesis - technology review and current scenario. Renew Sustain Energy Rev 2016;58:267–86. https://doi.org/10.1016/j.rser.2015.12.143.

[60] Marchese M, Heikkinen N, Giglio E, Lanzini A, Lehtonen J, Reinikainen M. Kinetic study based on the carbide mechanism of a Co-Pt/γ-Al2 O3 Fischer–Tropsch catalyst tested in a laboratory-scale tubular reactor. Catalysts 2019;9(9). https://doi.org/10.3390/catal9090717.

[61] Vedachalam S, Boahene P, Dalai AK. Production of jet fuel by hydrorefining of Fischer-Tropsch wax over Pt/Al-TUD-1 bifunctional catalyst. Fuel 2021;300 (February):121008. https://doi.org/10.1016/j.fuel.2021.121008.

[62] Catalysts P. Hydrocracking of heavy Fischer – Tropsch wax distillation; 2021.

[63] Rojas Michaga MF, Michailos S, Akram M, Cardozo E, Hughes KJ, Ingham D, et al. Bioenergy with carbon capture and storage (BECCS) potential in jet fuel production from forestry residues: a combined Techno-Economic and Life Cycle Assessment approach. Energy Convers Manag 2022;255(November):115346. doi: 10.1016/j.enconman.2022.115346.

[64] von Hepperger F. Master thesis implementation of water electrolysis in Växjö's combined heat and power plant and the use of excess heat. A techno-economic analysis.

[65] Li H, Svendsen S, Gudmundsson O, Kuosa M, Rämä M, Sipilä K, et al. Low temperature district heating for future energy systems; 2017. doi: 10.1016/j.egypro.2018.08.224.

[66] Skuma. Is London tap water safe?-Statistics; 2021. https://www.skumawater.com/is-london-tap-water-safe (accessed Jul. 21, 2022).

[67] Aline Noutcha ME, Damiete O, Johnny Jr M, Ngozi O, Ezera CU, Okiwelu SN. Quantity and quality of water condensate from air conditioners and its potential uses at the University of Port Harcourt, Nigeria). Pelagia Res Libr Adv Appl Sci Res 2016;7(6):45–8.

[68] CheCalc. Cooling tower makeup water; 2023. https://checalc.com/solved/ctmakeup.html (accessed Jan. 03, 2023).

[69] JMP. Cooling tower and condenser water design part 9: controlling cycles of concentration. https://jmpcoblog.com/hvac-blog/cooling-tower-and-condenser-water-design-part-9-controlling-cycles-of-concentration (accessed Jan. 04, 2023).

[70] Albarelli JQ, Onorati S, Caliandro P, Peduzzi E, Meireles MAA, Marechal F, et al. Multi-objective optimization of a sugarcane biorefinery for integrated ethanol and methanol production. Energy 2017;138:1281–90. https://doi.org/10.1016/j.energy.2015.06.104.

[71] König DH, Baucks N, Dietrich RU, Wörner A. Simulation and evaluation of a process concept for the generation of synthetic fuel from CO2 and H2. Energy 2015;91:833–41. https://doi.org/10.1016/j.energy.2015.08.099.

[72] Diederichs GW, Ali Mandegari M, Farzad S, Görgens JF. Techno-economic comparison of biojet fuel production from lignocellulose, vegetable oil and sugar cane juice. Bioresour Technol 2016;216:331–9. https://doi.org/10.1016/j.biortech.2016.05.090.

[73] Davis R, Tao L, Tan ECD, Biddy MJ, Beckham GT, Scarlata C, et al. Process design and economics for the conversion of lignocellulosic biomass to hydrocarbons: dilute-acid and enzymatic deconstruction of biomass to sugars and biological conversion of sugars to hydrocarbons. National Renewable Energy Laboratory-NREL, no. October 2013; 2013. p. 147. doi: 10.2172/1107470.

[74] Humbird D, Davis R, Tao L, Kinchin C, Hsu D, Aden A, et al. Process design and economics for biochemical conversion of lignocellulosic biomass to ethanol: dilute-acid pretreatment and enzymatic hydrolysis of corn Stover. National Renewable Energy Laboratory, no. May; 2011. p. 1–147. doi: 10.2172/1107470.

[75] Swanson RM, Platon A, Satrio JA, Brown RC. Techno-economic analysis of biomass-to-liquids production based on gasification scenarios. ACS National Meeting Book of Abstracts, no. November; 2009.

[76] Michailos S, Emenike O, Ingham D, Hughes KJ, Pourkashanian M. Methane production via syngas fermentation within the bio-CCS concept: a techno-economic assessment. Biochem Eng J 2019;150(May):107290. https://doi.org/10.1016/j.bej.2019.107290.

[77] Michailos S, Parker D, Webb C. A multicriteria comparison of utilizing sugar cane bagasse for methanol to gasoline and butanol production. Biomass Bioenergy 2016;95:436–48. https://doi.org/10.1016/j.biombioe.2016.06.019.

[78] National Academies. Negative emissions technologies and reliable sequestration; 2019. doi: 10.17226/25259.

[79] Young J, McQueen N, Charalambous C, Foteinis S, Hawrot O, Ojeda M, et al. The cost of direct air capture and storage: the impact of technological learning, regional diversity, and policy. ChemRxiv Preprint; 2022. p. 1–37.

[80] Peters MS, Timmerhaus KD, West RE. Plant design and economics for chemical engineers. 5th ed.; 2003.

[81] Michailos S, Walker M, Moody A, Poggio D, Pourkashanian M. A techno-economic assessment of implementing power-to-gas systems based on biomethanation in an operating waste water treatment plant. J Environ Chem Eng 2021;9(1):104735. https://doi.org/10.1016/j.jece.2020.104735.

[82] Eurostat. Electricity prices components for non-household consumers - annual data (from 2007 onwards); 2022. https://ec.europa.eu/eurostat/databrowser/view/NRG_PC_205_C_custom_3590784/default/table?lang=en (accessed Oct. 15, 2022).

[83] GOV.UK. Energy Security Bill factsheet: Network charging compensation scheme for energy intensive industries (added 9 May 2023); May 29, 2023. https://www.gov.uk/government/publications/energy-security-bill-factsheets/energy-security-bill-factsheet-network-charging-compensation-scheme-for-energy-intensive-industries (accessed Jun. 14, 2023).

[84] Grubb M, Drummond P. UK industrial electricity prices: competitiveness in a low carbon world; 2018. Accessed: Jun. 15, 2023. [Online]. Available: https://www.ucl.ac.uk/bartlett/sustainable/sites/bartlett/files/uk_industrial_electricity_prices_-_competitiveness_in_a_low_carbon_world.pdf.

[85] Peters MS, Timmerhaus KD. Plant design and economics for chemical engineers; 1991. doi: 10.1080/00137915908965075.

[86] Michailos S, Walker M, Moody A, Poggio D, Pourkashanian M. Biomethane production using an integrated anaerobic digestion, gasification and CO2 biomethanation process in a real waste water treatment plant: a techno-economic assessment. Energy Convers Manag 2020;209(February):112663. https://doi.org/10.1016/j.enconman.2020.112663.

[87] Office for National Statistics. A01: summary of labour market statistics - office for national statistics. https://www.ons.gov.uk/employmentandlabourmarket/peopleinwork/employmentandemployeetypes/datasets/summaryoflabourmarketstatistics (accessed May 12, 2021).

[88] Marchese M, Buffo G, Santarelli M, Lanzini A. CO 2 from direct air capture as carbon feedstock for Fischer-Tropsch chemicals and fuels: energy and economic analysis. J CO2 Util 2021;46:101487. https://doi.org/10.1016/j.jcou.2021.101487.

[89] Baumann H, Tillman A-M. The Hitch Hiker's guide to LCA; 2004.

[90] Pavlenko N, Searle S. "ICCT working paper: assessing the sustainability implications of alternative aviation fuels; 2021.

[91] Majer S, Oehmichen K, Moosmann D, Dbfz HS, Sailer K, Matosic M, et al. D5. 1 Assessment of integrated concepts and identification of key factors and drivers, no. 857796; 2021.

[92] TransportPolicy.net. US: fuels: renewable fuel standard | Transport policy. https://www.transportpolicy.net/standard/us-fuels-renewable-fuel-standard/(accessed Dec. 20, 2021).

[93] ASTM. Standard specification for aviation turbine fuel containing synthesized hydrocarbons; 2019. doi: 10.1520/D1655-10.2.

[94] Argonne National Laboratory. Life cycle analysis of alternative aviation fuels in GREET. Chicago; 2012.

[95] Unnasch S, Riffel B, Center VNTS, Life Cycle Associates LLC, Administration FA. Review of jet fuel life cycle assessment methods and sustainability metrics. 2015; 298(0704):123.

[96] Hermansson F, Janssen M, Svanström M. Allocation in life cycle assessment of lignin. Int J Life Cycle Assess 2020;25(8):1620–32. https://doi.org/10.1007/s11367-020-01770-4.

[97] Von Der Assen N, Jung J, Bardow A. Life-cycle assessment of carbon dioxide capture and utilization: avoiding the pitfalls. Energy Environ Sci 2013. https://doi.org/10.1039/c3ee41151f.

[98] Kolosz BW, Luo Y, Xu B, Maroto-Valer MM, Andresen JM. Life cycle environmental analysis of 'drop in' alternative aviation fuels: a review. Sustain Energy Fuels 2020;4(7):3229–63. https://doi.org/10.1039/c9se00788a.

[99] De Jong S, Antonissen K, Hoefnagels R, Lonza L, Wang M, Faaij A, et al. Life-cycle analysis of greenhouse gas emissions from renewable jet fuel production. Biotechnol Biofuels 2017;10(1):1–18. https://doi.org/10.1186/s13068-017-0739-7.

[100] Garcia-Teruel A, Rinaldi G, Thies PR, Johanning L, Jeffrey H. Life cycle assessment of floating offshore wind farms: An evaluation of operation and maintenance. Appl Energy 2022;307(September):118067. doi: 10.1016/j.apenergy.2021.118067.

[101] NREL. Wind LCA harmonization. 2013;2012(Awea):2. doi: 10.1111/j.1530-9290.2012.00464.x/pdf.

[102] Koj JC, Wulf C, Schreiber A, Zapp P. Site-dependent environmental impacts of industrial hydrogen production by alkaline water electrolysis. Energies (Basel) 2017;10(7). doi: 10.3390/en10070860.

[103] Delpierre M. An ex-ante LCA study on wind-based hydrogen production in the Netherlands. TU Delft Technology, Policy and Management; August, 2019.

[104] Terlouw T, Treyer K, Bauer C, Mazzotti M. Life cycle assessment of direct air carbon capture and storage with low-carbon energy sources. Environ Sci Technol 2021;55(16):11397–411. https://doi.org/10.1021/acs.est.1c03263.

[105] Ecoinvent. Market for kerosene EcoQuery - Dataset Details (UPR); 2017. https://v36.ecoquery.ecoinvent.org/Details/ShowUndefined/edcee36f-755b-49eb-b0c5-802debd94874 (accessed Jul. 15, 2021).

[106] Cherubini F, Bird ND, Cowie A, Jungmeier G, Schlamadinger B, Woess-Gallasch S. Energy- and greenhouse gas-based LCA of biofuel and bioenergy systems: key issues, ranges and recommendations. Resour Conserv Recycl 2009;53(8):434–47. https://doi.org/10.1016/j.resconrec.2009.03.013.

[107] AACE International. Recommended practice no. 18R-97: cost estimate classification system, Rev March 1, 2016; 2016. p. 10.

[108] Lamers P, Tan ECD, Searcy EM, Scarlata CJ, Cafferty KG, Jacobson JJ. Strategic supply system design - a holistic evaluation of operational and production cost for a biorefinery supply chain. Biofuels Bioprod Biorefin 2015;9(6):648–60. https://doi.org/10.1002/bbb.1575.

[109] Abdin Z, Webb CJ, Gray EMA. Modelling and simulation of an alkaline electrolyser cell. Energy 2017;138:316–31. https://doi.org/10.1016/j.energy.2017.07.053.

[110] Kojima H, Matsuda T, Matsumoto H, Tsujimura T. Development of dynamic simulator of alkaline water electrolyzer for optimizing renewable energy systems. J Int Council Electr Eng 2018;8(1):19–24. https://doi.org/10.1080/22348972.2018.1436931.

[111] Tijani AS, Yusup NAB, Rahim AHA. Mathematical modelling and simulation analysis of advanced alkaline electrolyzer system for hydrogen production. Proc Technol 2014;15:798–806. https://doi.org/10.1016/j.protcy.2014.09.053.

[112] Sánchez M, Amores E, Abad D, Rodríguez L, Clemente-Jul C. Aspen Plus model of an alkaline electrolysis system for hydrogen production. Int J Hydrogen Energy 2020;45(7):3916–29. https://doi.org/10.1016/j.ijhydene.2019.12.027.

[113] Rahman NA, Jose Jol C, Linus AA, Rozellia Kamel Sharif DS, Ismail V. Fischer Tropsch water composition study from distillation process in gas to liquid technology with ASPEN simulation. Case Stud Chem Environ Eng 2021;3. doi: 10.1016/j.cscee.2021.100106.

[114] Zang G, Sun P, Elgowainy AA, Bafana A, Wang M. Performance and cost analysis of liquid fuel production from H2and CO2based on the Fischer-Tropsch process. J CO2 Util 2021;46(February):101459. https://doi.org/10.1016/j.jcou.2021.101459.

[115] Bos MJ, Kersten SRA, Brilman DWF. Wind power to methanol: renewable methanol production using electricity, electrolysis of water and CO2 air capture. Appl Energy 2020;264(August 2019):114672. https://doi.org/10.1016/j.apenergy.2020.114672.

[116] Elfving J, Bajamundi C, Kauppinen J, Sainio T. Modelling of equilibrium working capacity of PSA, TSA and TVSA processes for CO2 adsorption under direct air capture conditions. J CO2 Utiliz 2017;22:270–7. doi: 10.1016/j.jcou.2017.10.010.

[117] S. I. für Z. S. S. W. I. für K. U. E. W. Deutsches Zentrum für Luft und Raumfahrt (DLR). MENA Fuels: Multikriterielle Bewertung von Bereitstellungstechnologien synthetischer Kraftstoffe, Teilbericht Nr. 3 (D2.1); 2021.

[118] Jiang L, Liu W, Wang RQ, Gonzalez-diaz A, Rojas-michaga MF, Michailos S, et al. Sorption direct air capture with CO 2 utilization. Prog Energy Combust Sci 2023; 95(January):101069. https://doi.org/10.1016/j.pecs.2022.101069.

[119] Price of offshore wind power falls to cheapest ever level in UK | Wind power | The Guardian. https://www.theguardian.com/environment/2022/jul/08/price-offshore-wind-power-falls-cheapest-ever-level-uk (accessed Feb. 22, 2023).

[120] Liu CM, Sandhu NK, McCoy ST, Bergerson JA. A life cycle assessment of greenhouse gas emissions from direct air capture and Fischer-Tropsch fuel production. Sustain Energy Fuels 2020;4(6):3129–42. https://doi.org/10.1039/c9se00479c.

[121] The Royal Society. Net zero aviation fuels: resource requirements and environmental impacts, 2023. Accessed: Apr. 24, 2023. [Online]. Available: https://royalsociety.org/-/media/policy/projects/net-zero-aviation/net-zero-aviation-fuels-policy-briefing.pdf.

[122] Rogers A, Parson O. GridCarbon: a smartphone app to calculate the carbon intensity of the UK electricity grid; 2047. p. 2–5.

[123] ESO. ESO data portal: ESO carbon intensity balancing actions methodology - dataset| National Grid Electricity System Operator. https://data.nationalgrideso.com/carbon-intensity1/carbon-intensity-of-balancing-actions/r/eso_carbon_intensity_balancing_actions_methodology#next (accessed Mar. 02, 2023).

[124] International Civil Aviation Organization. Guidance on potential policies and coordinated approaches for the deployment of sustainable aviation fuels; 2022. Accessed: Apr. 24, 2023. [Online]. Available: https://www.icao.int/environmental-protection/Documents/SAF/Guidance %20on %20SAF %20policies %20- %20Version %201.pdf.

[125] AVFUEL. Avfuel's Carbon Offset Program. https://www.avfuel.com/Fuel/Alternative-Fuels/Carbon-Offset (accessed Mar. 01, 2023).

[126] IATA. IATA - Fuel Price Monitor; 2021. https://www.iata.org/en/publications/economics/fuel-monitor/(accessed Apr. 28, 2021).

[127] Department for Transport. Pathway to net zero aviation: developing the UK sustainable aviation fuel mandate A second consultation on reducing the greenhouse gas emissions of aviation fuel in the UK; 2023. [Online]. Available: www.nationalarchives.gov.uk/doc/opengovernment-licence/version/3/.

[128] E. & I. S. Department for Business. Hydrogen production costs 2021; 2021. Accessed: Apr. 24, 2023. [Online]. Available: https://assets.publishing.service.gov.uk/government/uploads/system/uploads/attachment_data/file/1011506/Hydrogen_Production_Costs_2021.pdf.